Journal of Hydrology 602 (2021) 126761

Contents lists available at ScienceDirect

Journal of Hydrology

journal homepage: www.elsevier.com/locate/jhydrol

Revisiting the Rainfall Anomaly Index to serve as a Simplified Standardized Precipitation Index

Tayeb Raziei

Soil Conservation and Watershed Management Research Institute (SCWMRI), Agricultural Research, Education and Extension Organization (AREO), Tehran, Iran

ARTICLE INFO

This manuscript was handled by Marco Borga, Editor-in-Chief, with the assistance of Eylon Shamir, Associate Editor

Keywords:
Drought
Probability of zero precipitation
Probability density function
SPI
RAI
SSPI
Iran

ABSTRACT

The Rainfall Anomaly Index (RAI) is revisited herein as an alternative to the Standardized Precipitation Index (SPI), taking into account different time scales and the probability of zero precipitation as in the SPI procedure. To evaluate the performance of the modified RAI that stands as a Simplified Standardized Precipitation Index (SSPI), both indices were computed for 45 stations distributed across diverse climates of Iran. The resulted time series and frequency distribution of the indices values between different dry/wet classes were statistically compared. The results show a very strong association between the two indices at all stations and time scales, particularly at longer time scales. The spatial distribution of the correlation coefficient (R) computed between the two indices depicts large R values across Iran, particularly over northern and western Iran where precipitation is distributed more regularly throughout the year. The spatial distribution of the Shapiro-Wilks (S-W) normality test computed for all studied stations and time scales show values larger than 0.96 in northern and western Iran and lower values ranging from 0.82 to 0.96 for a few stations scattered in eastern, central, and southern Iran. This indicated that both indices have a closer distribution to the standard normal distribution in northern and western Iran where precipitation is less skewed. However, SSPI shows a lower S-W test than the SPI for some stations scattered over central-eastern Iran, which is an indication of its higher deviation from the normal distribution. The comparison of the frequency distribution of the indices values between different dry/wet classes also reveals a very strong association between the two indices, as indicated by very high values of contingency coefficient and Cramér's **V** statistic for all time scales at the studied stations. SSPI is simpler in calculation than the SPI and permits for missing data and large numbers of zero values in the data records, which is very common in arid and hyper-arid climates. Thus, SSPI is preferred over SPI when the length of data records is short or contains a large number of zero values for which SPI is incomputable or unreliable.

1. Introduction

Several drought indices are proposed for drought monitoring from which the Palmer Drought Severity Index (PDSI) (Palmer, 1965), the Standardized Precipitation Index (SPI) (Mckee et al., 1993), and the Standardized Evapotranspiration Index (SPEI) (Vicente-Serrano et al., 2010) are generally accepted and widely used all over the world. The Australian Drought Watch System uses the decile index (Gibbs and Maher, 1967) as the meteorological drought index. It is a rank-based drought index with a relatively simple calculation procedure and fewer assumptions than the PDSI (Hayes et al., 2011), requiring only precipitation as the input.

Undoubtedly, the SPI is the most robust and effective widely used drought index that enjoys several advantages over many indices introduced in the literature (Vicente-Serrano, 2006). Hayes et al. (1999) discussed the advantages and disadvantages of SPI in characterizing drought events. According to Hayes et al. (1999), SPI requires only precipitation that is available with a much finer spatial and temporal coverage across the land areas of the globe. For calculating SPI, the most suited probability distribution function (PDF) is first fitted to the precipitation time series aggregated at different timescales and then the resulted cumulative probability distribution (CDF) is normalized to obtain the index value. The SPI can be temporally and spatially comparable if a uniform calculation process is implemented, otherwise, comparing the SPI values will not be easy if different probability distribution functions are used for different locations. This makes the SPI not affected by geographical or topographical differences (Hayes et al., 1999; Lana et al., 2001). The World Meteorological Organization (Hayes et al., 2011; WMO, 2006) has recommended the SPI as a generally accepted index for drought monitoring and characterization in all

E-mail address: tayebrazi@yahoo.com.

https://doi.org/10.1016/j.jhydrol.2021.126761
Received 9 March 2021; Received in revised form 31 May 2021; Accepted 27 July 2021
Available online 3 August 2021

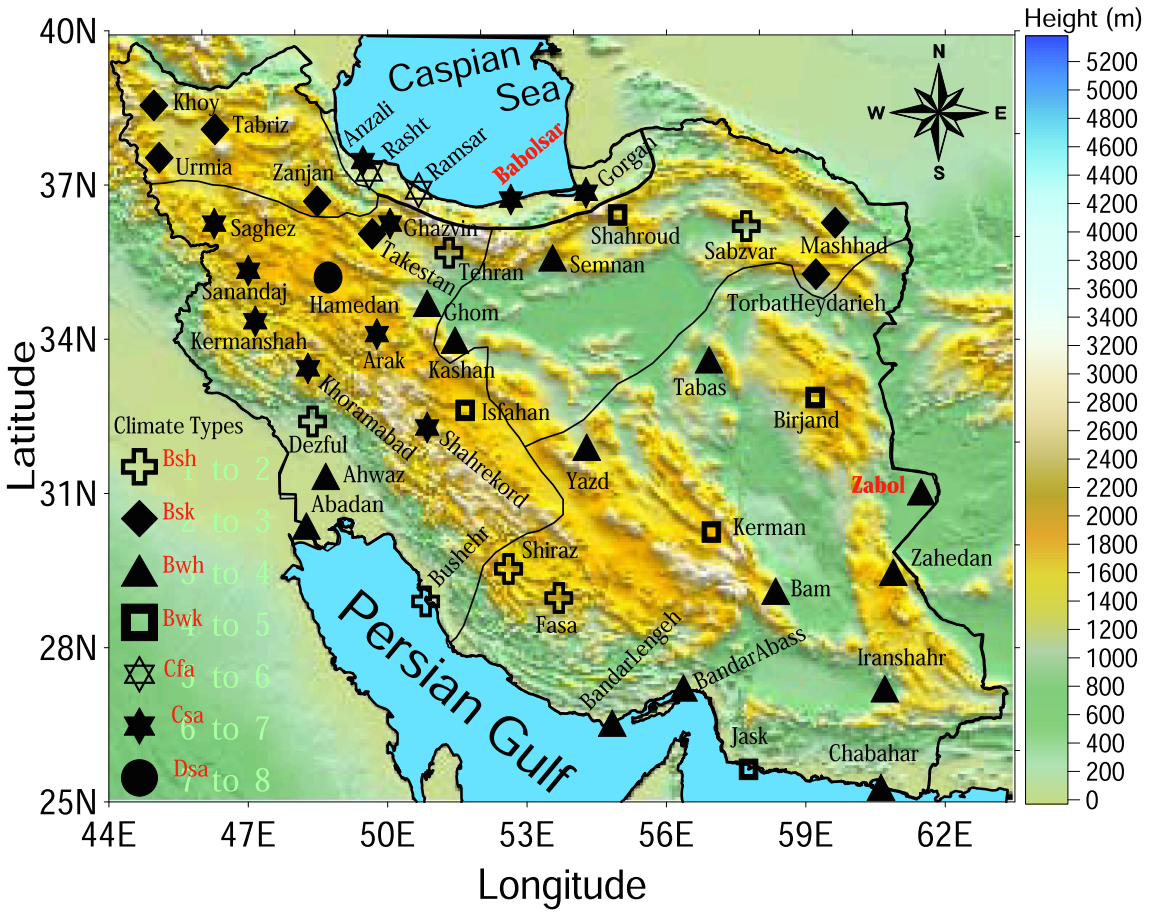

Fig. 1. The DEM of Iran with the spatial distribution of 45 selected stations overlaid. The climate types of the stations determined by Raziei (2017) and the boundary of the five precipitation sub-regions of Iran identified by Raziei (2018) are also illustrated. The two example stations of Babolsar and Zabol used to evaluate the performance of the proposed index are in red.

climatic regions of the world. Being based upon the probability of precipitation values accumulated over different time scales ranging from 1 to 72 months (Edwards and McKee, 1997), SPI is suitable to identify all types of droughts, namely, the meteorological, hydrological, agricultural, and socio-economic droughts. However, according to Guttman (1994) and Guttman (1999), the practical range of SPI time scales is 1- to 24-month if one notes that around 50–60 years of data is required for a confidential SPI computation. Therefore, unless 80–100 years of data is available, the sample size is too small and the statistical confidence of the probability estimates on the tails of the distribution becomes very weak for time scales beyond 24 month Svoboda et al. (2012). Guttman (1998) has recommended the SPI as the primary drought index due to its simpler computation procedure and spatially consistent (invariant) in its interpretation and probabilistic so that it can be used in risk and decision analysis.

Due to its advantages mentioned above, SPI was extensively used for drought analysis and characterization in different areas around the globe, including the U.S.A. (Hayes et al., 1999), Europe (Lloyd-Hughes and Saunders, 2002), South Africa (Rouault and Richard, 2003), Hungary (Domonkos, 2003), Italy (Bonaccorso et al., 2003), East Africa (Ntale and Gan, 2003), Greece (Tsakiris and Vangelis, 2004) and Korea (Min et al., 2003). However, according to Hayes et al. (1999), the SPI has three potential disadvantages: a) the assumption of finding a suitable theoretical probability distribution to fit the raw precipitation is largely dependent on the quantity and reliability of the data used to fit the distribution (Guttman, 1999; Quiring, 2009); b) equal value of SPI at two different locations does not necessarily imply an equal water deficit at the locations (Wu et al., 2007), indicating that the SPI is not capable of distinguishing drought-prone regions from other areas, c) when applying the SPI at short time scales in regions with highly seasonal precipitation, misleadingly large positive or negative SPI values may result, particularly in arid and semi-arid regions having many months with zero precipitation (Wu et al., 2007). The SPI is also based on the assumption of fitting precipitation data to a given PDF (Lloyd-Hughes and Saunders, 2002; Wu et al., 2007) which is valid when long-term data records are available that is not always the case in arid and hyper-arid climates, particularly in the seasons with many zero precipitation values; thus, resulting in less reliable SPI values at shorter time scales. By proposing a non-parametric normalization procedure for SPI computation, Farahmand and AghaKouchak (2015) attempted to overcome such a conceptual drawback (Raible et al., 2017). The proposed approach is a rank-based method that simply transforms the plotting positions to the standard normal distribution (Farahmand and AghaKouchak, 2015) to directly describes any sample at hand independent of its properties, and without requiring testing for the goodness of fit (Tijdeman et al., 2020). As another disadvantage, SPI also does not assumes temporal stationarity over the period for which it is calculated; therefore, its robustness in drought characterization under a changing climate is not clear (Seneviratne et al., 2012).

Like the decile index (Gibbs and Maher, 1967), the Rainfall Anomaly Index (RAI) developed by Van-Rooy (1965) incorporates a ranking procedure to assign magnitudes to positive and negative precipitation anomalies (Keyantash and Dracup, 2002), utilizing a normalization procedure more simpler than that used in SPI computation. Olukayode Oladipo (1985) found insignificant differences between RAI and the more complicated drought indices like PDSI in Nebraska State, USA.

Likewise, Keyantash and Dracup (2002) found a very strong association between RAI and SPI time series in two climate divisions of Oregon State, USA. Loukas et al. (2003) also found RAI and SPI time series highly comparable in Greece. More recently, Hänsel et al. (2016) evaluated the suitability of a modified version of RAI as an alternative to SPI in assessing future precipitation conditions in central Europe and found it highly correlated with SPI. As stated by Hänsel et al. (2016), RAI offers a higher degree of transparency and tractability and has a lower degree of sophistication than the SPI, concerning the evaluation criteria for drought indices proposed by Keyantash and Dracup (2002). It is also computationally less demanding than SPI but with comparable performance as reported by the aforementioned studies.

The aforementioned studies have evaluated the performance of RAI in small homogenous areas with humid to moderate climates where precipitation is less skewed compared to arid and hyper-arid climates characterized by periods with a high probability of zero precipitation (PZP). However, although Loukas et al. (2003) have already tested RAI in a few Greek stations with temperate climate where zero precipitation values during summer month are common, there is no information regarding the performance of RAI in arid and hyper-arid climates where precipitation is highly skewed and zero precipitation values dominated its lengthy warm dry period (Raziei, 2021). Therefore, this study proposes some modifications to RAI and evaluates its performance in diverse climates of Iran that includes arid and hyper-arid climates. The proposed modifications make the index a better tool for drought monitoring in arid and hyper-arid climates of the world where precipitation data is either short, incomplete, or contains very high PZP (Raziei, 2021) with which computing SPI is impossible or unreliable. The modified RAI is expected to serve as a Simplified Standardized Precipitation Index (SSPI), as it is very simple in computation, and requires less statistical assumptions and computational demands while resulting in values highly comparable with SPI values. It is particularly superior over SPI for application in arid and hyper-arid climates, particularly at shorter time scales when the existence of very high PZP makes computing SPI impossible or unreliable.

2. Materials and methods

2.1. Data

Fig. 1 illustrates the spatial distribution of 45 Iranian first-order synoptic stations used in this study. The stations were selected based on the availability of data records with no missing values for a period as long as possible. These criteria made the selected stations denser in western and northwestern Iran and scattered in central-eastern Iran where hosted large inhabitant areas including several deserts of Iran (see Fig. 1). The selected stations monitored by the Iranian Meteorological Organization (IRIMO) have complete data records from 1971 to 2018 with an acceptable distribution across diverse climate types of Iran defined by Raziei (2017) based on the Köppen-Geiger climate classification system. The selected stations contain an adequate number of representative stations for each of the five main precipitation subregions of Iran characterized by different monthly precipitation variability (Raziei, 2018) and dry/wet periods (Raziei et al. 2011, 2013; Raziei et al. 2010). The monthly precipitation records of the selected stations, downloaded from the IRIMO website at http://www.irimet.net, possessed a few missing values only in two of the stations that were estimated by establishing a linear regression between the station with missing values and their neighboring stations. Adopting the rationale simple linear imputation process in this study is reasonable since the percentage of missing values requiring imputation is tiny. However, utilizing non-linear machine learning methods including the support vector machines and artificial neural network algorithms is preferable when data have more missing values (Richman et al., 2009).

Table 1
The classification of the RAI index used by Van-Rooy (1965), and the RAI/SPI classification system developed by Hänsel et al. (2016).

RAI	RAI/SPI	Class description
≥3	≥2	Extremely wet
2.00 to 2.99	1.50 to 1.99	Very wet
1.00 to 1.99	1.00 to 1.49	Moderately wet
0.50 to 0.99	0.50 to 0.99	Slightly wet
−0.49 to 0.49	−0.49 to -0.49	Near normal
−0.99 to −0.50	−0.99 to −0.50	Slightly dry
−1.99 to −1.00	−1.49 to −1.00	Moderately dry
−2.99 to −2.00	−1.99 to −1.50	Very dry
≤ −3.00	≤ −2.00	Extremely dry

2.2. SPI computation

The SPI is calculated by fitting a probability distribution function to the frequency distribution of precipitation data aggregated at any desired time scale. In other words, computing SPI begins with determining a probability density function that best describes the aggregated precipitation time series at a given time scale. Then, the determined cumulative probability of the observed precipitation values is converted to a standard normal distribution to obtain the SPI values (Edwards and McKee, 1997). In the present study, SPI is computed by fitting a Gamma PDF to precipitation aggregated at all the time scales considered. Although Raziei (2021) has identified the Pearson Type III distribution as the most appropriate distribution function in fitting precipitation aggregated at all considered time scales throughout Iran, the Gamma PDF was intentionally used herein because it is extensively used in Iran as it is the default PDF of many codes available for SPI computation (Raziei, 2021). Nonetheless, Raziei (2021) showed that Gamma best fitted monthly precipitation over most parts of Iran and identified it as one of the PDFs with the lowest goodness of fit rejection rate for all considered time scales.

For the present study, besides the monthly precipitation series of each calendar month as the representative of one-month time scale, time series of longer precipitation aggregations of 3-, 6-, 9-, 12-, and 24-months were also constructed for computing SPI at 1-, 3-, 6-, 9-, 12-, and 24-month time scales. The longer than 1-month aggregations are averages of the monthly values in the aggregation duration, ending in each of the 12 calendar months of the year. The shorter time scales (1-, 3-, and 6-month) are usually used for monitoring meteorological and agricultural droughts and the longer ones (9-, 12-, and 24-month) are useful for monitoring hydrological droughts (Edwards and McKee, 1997) that includes groundwater and surface water (Van Lanen and Peters 2000).

2.3. RAI computation

Similar to the decile index (Gibbs and Maher, 1967), RAI developed by Van-Rooy (1965) is a rank-based drought index that incorporates a ranking procedure to assign magnitudes to positive and negative precipitation anomalies (Keyantash and Dracup, 2002). The RAI index is computed as below.

$$\mathrm{RAI} = \pm 3\frac{P_i - \bar{P}}{\bar{E} - \bar{P}} \quad (1)$$

In Eq. (1), P_i is the sequence of measured precipitation at the time i , $\bar{P}$ is average precipitation, $\bar{E}$ is average of 10 extrema and ± 3 is the prefix used to limits the lower and upper bounds of the anomalies. This standardization follows the unity-based feature scaling (Aksoy and Haralick, 2001; Khansalari et al., 2018) to asymmetrically distribute the original anomalies between the predefined limits (-3 and + 3). For positive anomalies (i.e., P_i-$\bar{P}$ greater than 0), the prefix is positive (i.e., 3) and $\bar{E}$ is the average of the 10 highest precipitation values on record; for negative anomalies (i.e., P_i-$\bar{P} < 0$), the prefix is negative (i.e., −3) and

the average of 10 lowest measurements are used (Keyantash and Dracup, 2002). However, calculating $\bar{E}$ from the ten largest (smallest) precipitation values appear arbitrary. Van-Rooy (1965) chose 10 because he thought the average of 10 extremes could represent the mean conditions of an extremely dry year or extremely wet year (Shen et al., 2006). The index values are judged against a 9-member classification scheme as in Table 1 (left column), ranging from extremely wet (RAI $\geq$ 3) to extremely dry (RAI $\leq$ -3). This classification which is similar to that used by Gibbs and Maher (1967) to partition precipitation values between ten deciles is equally applicable to various lengths of drought, including flash droughts, meteorological drought, deep soil moisture drought, and hydrological drought defined with RAI computed at different time scales.

As demonstrated by Keyantash and Dracup (2002), Loukas et al. (2003), and Hänsel et al. (2016), Eq. (1) performs well in humid to moderate climates of the world where monthly precipitation distributed relatively regularly throughout the year, and the associated distribution is less skewed. For example, Keyantash and Dracup (2002) examined the performance of RAI in two climate divisions of Oregon State, USA, characterized by moist to moderate climates denoted as Köppen Csb climate type, , and found a very high correlation coefficient between SPI and RAI computed at 1-month time scale. Similarly, Loukas et al. (2003) have evaluated the performance of RAI in the Mediterranean climates of Greece that are classified as Csa, Csb, or Cfb Köppen climate types. However, despite that summer is dry and precipitation occurrence in some of their studied stations is less likely in that season, they found an excellent agreement between RAI and other drought indices in depicting drought and wet periods. Likewise, Hänsel et al. (2016) have assessed the performance of RAI in central Europe characterized by Köppen Cfb climate type. However, Eq. (1) does not perform well in most parts of Iran that are characterized by Bsk, Bsh, Bwh, and Bwk climate types (Raziei, 2017) as shown in Fig. 1. In such areas, the June-September period is totally dry with a very low chance of precipitation (Raziei, 2021). Hence, a very large proportion of monthly and seasonal aggregated precipitation time series is zero that often results in zero mean and median as the climate norm of the region (Raziei, 2021). In cases when PZP is $\geq$ 40%, very likely P, $\bar{P}$ and $\bar{E}$ become zero; and thus, computing RAI becomes impossible. This suggests taking into account the PZP of the dry months as the climate norm of the region for RAI computation.

Therefore, as in the SPI computation procedure, it is desirable to consider time scales and PZPs of the dry months in RAI computation. To consider the aforementioned issues in RAI computation, a few modifications outlined below are proposed.

1- Aggregate monthly precipitation data to any desire time scale as in the SPI procedure.
2- Compute the skewness of the aggregated monthly precipitation for a given time scale ended at each calendar month.
3- Reduce the skewness of the aggregated monthly precipitation series using the cube root transformation if its skewness is greater than 0.5 and the cube transformation (x^3) if it is less than -0.5.
4- Compute the anomalies of the transformed precipitation time series (Δ) for the aggregated transformed precipitation by subtracting P_i from $\bar{P}$ (*i.e.*,$P_i - \bar{P}$), where P_i is i_{th} transformed precipitation value and $\bar{P}$ is the median of the transformed series.
5- For each time scale ended at each 12 calendar month, rank the transformed data (P), remove duplicate values, and then compute the 5th, 50th, and 95th percentiles of the data.
6- Set the 5th and 95th percentiles of the ranked transformed data as the average of the bottom 5% precipitation records ($\bar{P}_B$) and the average of top 5% precipitation records ($\bar{P}_T$), respectively. Similarly, consider the 50th percentile as the median ($\bar{P}$) of the data. The logic behind using $\bar{P}_B$ and $\bar{P}_T$ (the 5th and 95th percentiles) as the threshold is that if 100 years of data records are used, then $\bar{P}_T$ is the mean of the 5 largest and $\bar{P}_B$ is the mean of the 5 smallest values of the data records (Shen et al., 2006). Using the lowest and highest percentiles will give more realistic results, particularly when the time series (P) is notably shorter than the ones Van-Rooy (1965) used in his analysis (Hänsel et al., 2016). Using the 5th and 95th percentiles in Eq. 2 as $\bar{P}_B$ and $\bar{P}_T$, respectively, causes the index values to exceed -3 and $+3$ limits. Instead, if the minimum and maximum of the data are used in Eq. 2 the index will reach –3.0 when P reaches $\bar{P}_B$ and will reach 3.0 when P reaches $\bar{P}_T$, and thus, the index values are confined between -3 and $+3$. Therefore, the original equation is

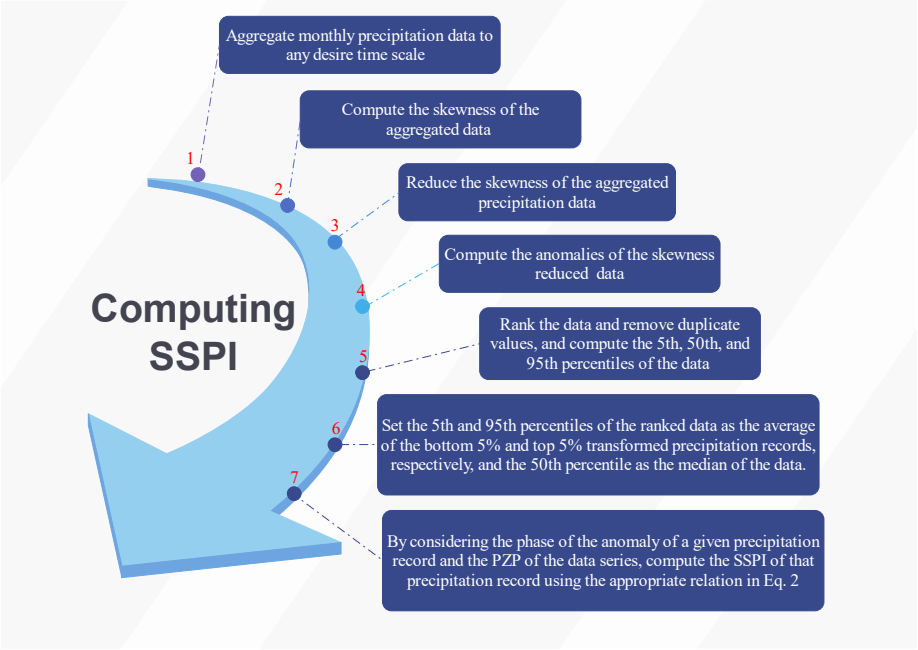

Fig. 2. The flowchart of computing SSPI.

Table 2
Computation procedure of the SSPI at 1-month time scale for January and August of Zabol station at the border with Afghanistan (see Figure 1).

Year	January				August			
	precipitation	transformed data	anomaly	SSPI	precipitation	transformed data	anomaly	SSPI
1971	3.0	1.4	−0.9	−1.7	0.0	0.0	0.0	0.0
1972	16.8	2.6	0.2	0.4	0.0	0.0	0.0	0.0
1973	0.4	0.7	−1.6	−3.0	0.0	0.0	0.0	0.0
1974	48.2	3.6	1.3	2.2	0.0	0.0	0.0	0.0
1975	70.0	4.1	1.8	3.0	0.0	0.0	0.0	0.0
1976	7.2	1.9	−0.4	−0.7	0.0	0.0	0.0	0.0
1977	19.4	2.7	0.4	0.6	0.3	0.7	0.7	3.0
1978	22.6	2.8	0.5	0.8	0.0	0.0	0.0	0.0
1979	5.4	1.8	−0.6	−1.1	0.0	0.0	0.0	0.0
1980	22.4	2.8	0.5	0.8	0.0	0.0	0.0	0.0
1981	22.4	2.8	0.5	0.8	0.0	0.0	0.0	0.0
1982	25.0	2.9	0.6	1.0	0.0	0.0	0.0	0.0
1983	0.4	0.7	−1.6	−3.0	0.0	0.0	0.0	0.0
1984	11.0	2.2	−0.1	−0.2	0.0	0.0	0.0	0.0
1985	11.6	2.3	−0.1	−0.1	0.0	0.0	0.0	0.0
1986	3.0	1.4	−0.9	−1.7	0.0	0.0	0.0	0.0
1987	0.4	0.7	−1.6	−3.0	0.0	0.0	0.0	0.0
1988	6.8	1.9	−0.4	−0.8	0.0	0.0	0.0	0.0
1989	0.9	1.0	−1.4	−2.6	0.0	0.0	0.0	0.0
1990	6.4	1.9	−0.5	−0.9	0.0	0.0	0.0	0.0
1991	13.7	2.4	0.1	0.1	0.0	0.0	0.0	0.0
1992	16.7	2.6	0.2	0.4	0.0	0.0	0.0	0.0
1993	25.6	2.9	0.6	1.0	0.0	0.0	0.0	0.0
1994	40.0	3.4	1.1	1.8	0.0	0.0	0.0	0.0
1995	6.2	1.8	−0.5	−0.9	0.0	0.0	0.0	0.0
Skewness	1.65	0.00	0.00	−0.12	4.69	4.69	4.69	4.69

slightly modified to confine the index between −3 and + 3 when using the 5th and 95th percentiles as $\bar{P}_B$ and $\bar{P}_T$.

Using a set of modifications described above, the modified RAI hereafter called SSPI can be computed as below for a certain month i.

$$\mathrm{SSPI}=\begin{cases} 3\left(\frac{P_i-\bar{P}}{\bar{P}_T-\bar{P}}+\left(\frac{P_i-\bar{P}}{\bar{P}_T-\bar{P}}-\frac{P_i-\bar{P}}{P_{Max}-\bar{P}}\right)\right) & if\ \ \Delta_i>0\ \ and\ \ PZP<40\% \\ -3\left(\frac{P_i-\bar{P}}{\bar{P}_B-\bar{P}}+\left(\frac{P_i-\bar{P}}{\bar{P}_B-\bar{P}}-\frac{P_i-\bar{P}}{P_{Min}-\bar{P}}\right)\right) & if\ \ \Delta_i\le 0\ \ and\ \ PZP<40\% \\ -3\frac{P_i-\bar{P}}{-(\max(P))-0} & if\ \ \max(P)>0\ \ and\ \ PZP\ge 40\% \\ -3\frac{P_i-\bar{P}}{-\varepsilon-0} & if\ \ \max(P)=0\ \ and\ \ PZP\ge 40\% \end{cases} \quad (2)$$

In Eq. (2), Δ_i is the anomaly value of the transformed observation i computed as $\Delta_i = P_i-\bar{P}$.

Since precipitation aggregated at various timescales are highly skewed in most of the studied stations , the median ($\bar{P}$) is used instead of the arithmetic mean of the precipitation time series P (Hänsel et al. 2016). Using the median is particularly more efficient than the mean of the data in dealing with precipitation time series of arid and hyper-arid climates where a majority proportion of precipitation records are zero (Raziei, 2021). In this modification, the PZP also makes a major role. The first and second relations of Eq. 2 are exactly those of the original equation of Van-Rooy (1965) that can be applied to the months and time scales with PZP < 40% when an adequate number of non-zero precipitation records is available for computing the 5th, 50th, and 95th percentiles of the data. Since the first part of these equations that uses the 5th and 95th percentiles to standardize the data does not bound the data between −3 and 3, the second part is added to standardize the data with its minimum and maximum, then subtract its result from the earlier part and adding the results to the original standardization in the first part of the relation to limit the outcome between −3 and 3. The proposed rescaling limits the SSPI values between the SPI range and obtains similar values and class frequencies as those of the SPI. Hänsel et al. (2016) have set the scaling factor of Eqs. (1) to 1.7 to limit the index values between the range of SPI values; assuming that it is an arbitrary value that can be adjusted to obtain RAI values in the range of any drought index with which RAI is comparing.

Here, the third and fourth relations of Eq. (2) are proposed to address the large proportion of zero values in arid and hyper-arid climates of the world that hinders computing SSPI with the first and second relations, since most likely the median of the data is zero for summer months. In such cases, when the maximum of the non-zero precipitation records denoted by max (P) is a positive integer (max (P) greater than 0) the SSPI is computed using the third relation. For example, when PZP ≥ 40% and max (P) is a positive integer, the third relation assigns 3.0 to that value as the maximum SSPI and smaller positive SSPI to all other non-zero precipitation values smaller than max (P). However, the third relation fails when all the time series are zero (i.e., PZP = 100%), and thus $\bar{P}=0$. In such cases, instead of max (P), an arbitrarily small positive quantity denoted by ε is used in the denominator of the fourth relation to avoid division by zero. The flowchart of the SSPI computation procedure is illustrated in Fig. 2 with a numerical example given in Table 2.

Table 2 shows the procedure of computing a 1-month time scale SSPI for January and August in Zabol station as the representatives of the wet and dry months of the station. Here only 25 years of data (1971-1995) is used to limit the size of the Table. As shown, the computed skewness of the precipitation time series of January is 1.65 that signals a highly skewed distribution. Since the skewness is positive and greater than 0.5 the time series was cube root transformed which reduced the skewness to zero which is an indication of the symmetrical distribution of the transformed series. The transformed series is then used to compute the anomalies by subtracting each value from the long-term mean of the transformed time series. After that, the transformed data is ranked and the 5_{th}, 50_{th}, and 95_{th} percentiles of the transformed data are computed and used in the first and second relations of Eq. 2 to compute SSPI as detailed above in step 6. As is seen, the skewness of both anomaly and SSPI time series for January are 0.0 and -0.12, respectively, implying that their distributions are quasi symmetrical. The right-hand part of the Table shows how the SSPI is computed for August when almost all the

time series is zero, except for the seventh record that equals 0.3 mm. As is seen the skewness of August is 4.69 and the cube root transformation was not able to reduce it anymore. Since most of the August precipitation time series is zero (PZP>40%) and the maximum of the transformed series (max (P)) is 0.7 the third relation was used for computing SSPI. This relation designates zero SSPI to all zero precipitation values (subtracting zero from zero) and the maximum positive SSPI to the single non-zero precipitation record. Note that when all the records are zero the fourth relation is used for computing the SSPI. It should also be noted that it is impossible to compute SPI for such a time series. SSPI is a standardized index that accounts for the PZP and the median of precipitation records and results in values that are highly comparable to SPI values in all climatic areas of Iran as described in the next sections. To have comparable frequencies of SPI and SSPI values in different classes, the classification system of Hänsel et al. (2016) shown in the middle column of Table 1 has been adopted. This classification system is a modification of the original classifications of Van-Rooy (1965) and Mckee et al. (1993).

2.4. Comparing SSPI with SPI

The performance of SSPI in different climate regions of Iran was evaluated against the SPI time series computed with both parametric and non-parametric (hereafter SPInp) approaches. However, for the sake of brevity, the comparison made between SSPI and SPInp was presented only for two example stations of Babolsar located along the Caspian Sea in the north and Zabol in southeast Iran where SSPI showed the highest and the lowest agreement with SPI, respectively. Babolsar climate type is Cfa (Raziei, 2017) which resembles the climates of the stations used by Keyantash and Dracup (2002), Loukas et al. (2003), and Hänsel et al. (2016) while Zabol station is considered as the representative of the hyper-arid climate of Iran with a climate type of Bwh (Raziei, 2017). The later station has a long dry period with very high PZPs. SSPI was primarily compared with SPI through Pearson correlation coefficient (R) and Spearman's rank correlation coefficient computed between the time series of SSPI and SPI indices computed at different time scales. However, due to the existence of a strong linear relationship between the indices at all studied stations and time scales, Spearman's rank correlation coefficient approaches to 1.0 at most of the studied stations, particularly for time scales larger than 3 month. Therefore, for assessing the degree of agreement between the indices the Pearson correlation coefficient was rather used since it shows a wider range of values over the stations that favors illustrating the inter-stations variation of correlation coefficient.

To assess the spatial variation of the R values over Iran characterized by different Köppen-Geiger climate types (Raziei, 2017), the computed R values for the studied stations distributed across Iran were mapped for all considered time scales. The consistency between the SSPI and SPI indices was also illustrated by comparing the time variability and PDF of the indices as well as the scatterplots of precipitation vs. the indices values for the two example stations of Babolsar and Zabol (see Fig. 1).

Because SPI values fit a typical normal distribution to define the number of standard deviations by which a normally distributed random variable deviates from its long-term mean (Guenang and Kamga, 2014), it is expected that the SPI values fall within one standard deviation in approximately 68% of the time, within two standard deviations 95% of the time, and within three standard deviations 99% of the time (Hayes et al., 1999). This feature enables SPI to represent both wetter and drier periods in the same way; meaning that an SPI value <-1.0 and < -2 occurs 16 and two to three times in 100 years, respectively, while an SPI of less than -3.0 occurs once in approximately 200 years (Hayes et al., 1999). Accordingly, since it is expected that the final SPI values follow a standard normal distribution it is reasonable to test whether the SPI values computed for a given station and time scale meet this assumption. For this purpose, the S-W test (Shapiro and Wilk, 1965; Stephens, 1974) was also used to examine whether the SPI values calculated through the equiprobability transformation (Wu et al., 2007) are normally distributed. The S-W test is based on the assumption that the SPI values should be normally distributed ($\mu = 0$, $\sigma = 1$) and independently sampled. However, the S-W test is strongest against short-tailed (platykurtic) and skewed distributions and weakest against symmetric moderately long-tailed (leptokurtic) distributions and also has issues with ties and extreme values (Royston, 1992, 1993). Therefore the S-W test used here is based on a method proposed by Wu et al. (2007) who used it in conjunction with two more criteria to guarantee that the examined series is normally distributed. This approach was also used by Naresh Kumar et al. (2009) to test the suitability of SPI values in arid regions with substantial zero precipitation values. Based on these criteria the distribution of the examined indices is non-normal when it's S–W test and the associated p-value is<0.96 and 0.10, respectively, and the absolute value of the index median is greater than 0.05; otherwise, the distribution is normal (Naresh Kumar et al., 2009; Stagge et al., 2015; Wu et al., 2007). When these three criteria are met simultaneously the normality assumption of the distribution is rejected. More recently, Stagge et al. (2015) and Svensson et al. (2017) have also used this test to evaluate the performance of different candidate distribution functions for SPI computation over Europe and the UK, respectively. As stated above, for application of the S-W test it is assumed that the data are independently sampled. Thus, to examine the assumption of whether the SPI and SSPI values are independently sampled, the autocorrelation of the indices time series of each station and time scale ended at each calendar month was computed. The result showed no significant autocorrelation for lags greater than 1 in any station and time scale, indicating that the indices values relative to all time scales and stations are independently sampled. In addition, the skewness and kurtosis of the indices time series were also computed for all considered stations and time scales to provide more insights on how far they are from normality. The normal quantile-quantile plots (q-q plot) were also provided for the two example stations to illustrate the closeness of their computed indices to the standard normal distribution.

Moreover, the frequencies of SPI and SSPI classes defined based on the nine anomaly classes shown in Table 1 were cross-tabulated to examine if they are comparable in partitioning the time series into different classes. The chi-square statistic of the contingency table established between the two indices and the associated p-value was used to determine if the relationship between the variables is significant at the 0.95 confidence level while the contingency coefficient (CC) and the Cramér's V statistic (Cramer, 1946) computed with the chi-square statistic were used to measure their degree of association. The CC and Cramér's V statistic (Cramer, 1946) defined in Eqs. (3) and (4), respectively, are chi-squared-based measures of association that define whether the two nominal variables or data sets are independent or dependent of each other. The values of these measures range between 0 and 1, where 0 indicating no association between the row and column variables of a contingency table and values close to 1 indicating a high degree of association between the variables.

$$CC = \sqrt{\frac{X^2}{n + X^2}} \tag{3}$$

$$V = \sqrt{\frac{X^2}{n.\min(r-1, c-1)}} \tag{4}$$

In Eqs. (3) and (4), n is the number of observations of SSPI/SPI time series classified between the classes, r and c are the numbers of rows and columns of the contingency table established between the indices frequency of cross-classification, and X^2 is the chi-square statistic that measures the statistical relationship between the variables in the cross-classification table.

Besides, as an illustrative example, the histograms of the frequency distribution of the SSPI and SPI values between the classes are illustrated for the two example stations.

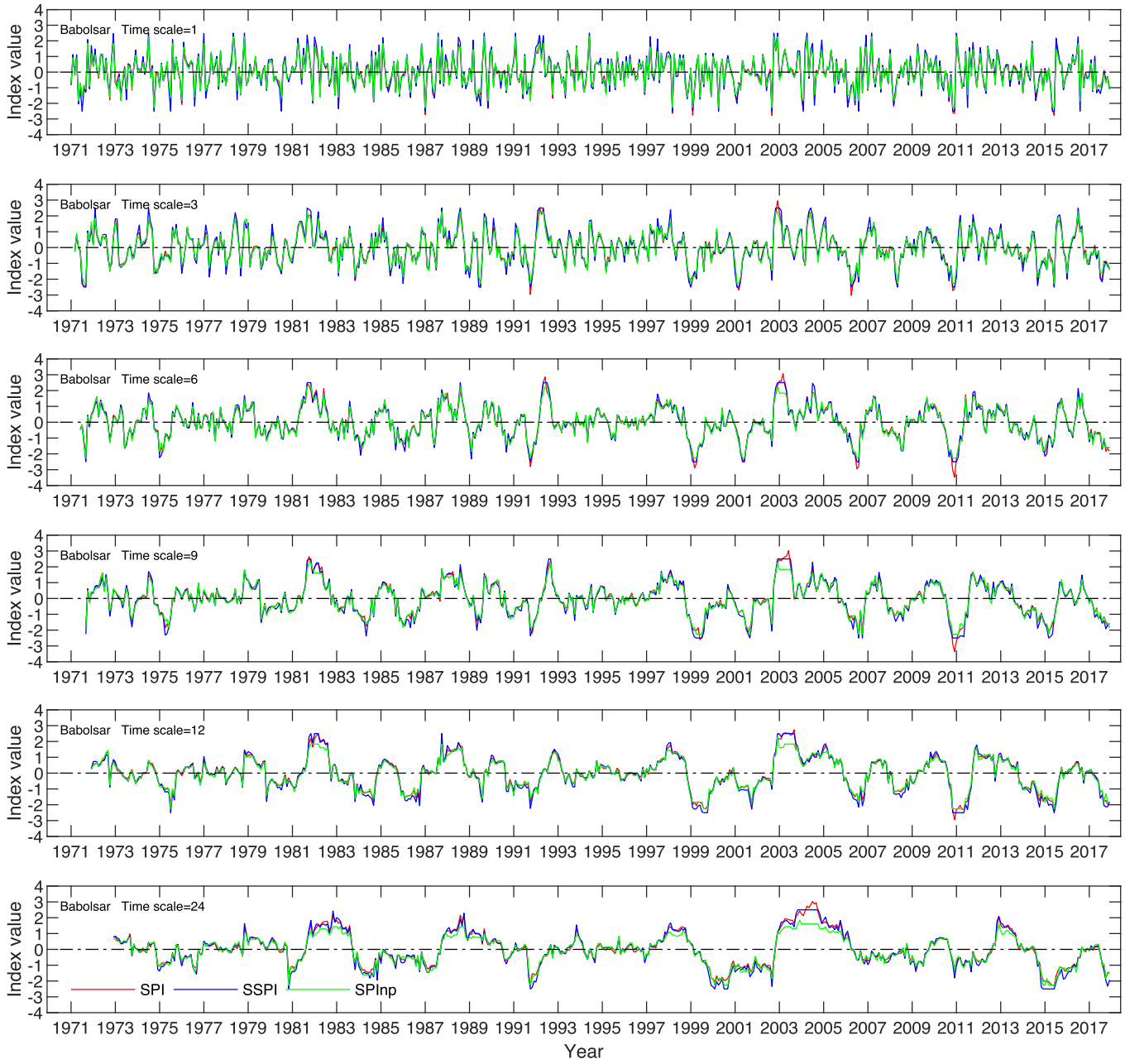

Fig. 3. Comparison of SPI, SPInp and SSPI time series of Babolsar station in the north of Iran computed at 1-, 3-, 6-, 9-, 12-, and 24-month time scales based upon 1971–2017 period.

3. Results

3.1. Comparing time variability of the indices

Fig. 3 shows the time variability of SPI and SSPI time series at Babolsar station in the north of Iran, computed at 1-, 3-, 6-, 9-, 12-, and 24-month time scales within the period 1971–2017. As it is seen, SSPI strongly co-vary with SPI (SPInp) at all time scales, particularly at longer ones. The R between the two indices is higher than 0.98 for 1- and 3-month time scales and higher than 0.99 for the rest of the time scales. This strong association between the two indices indicates that SSPI well represents the time variability and magnitudes of SPI at Babolsar station that has a Cfa climate type (Raziei, 2017). Similarly, Fig. 4 shows the time behavior of the indices for Zabol station in the southeast of Iran that has a Bwh climate type (Raziei, 2017). As it is evident, there is also a strong agreement between the three indices in Zabol station where it's very long dry period leads very high PZPs in shorter time precipitation aggregations. The R between the indices is 0.78, 0.84, and 0.92 for 1-, 3- and 6-month time scales, which is noticeably lower than those computed for Babolsar station at the same time scales. The observed lower correlation for these time scales at Zabol station is partly because SPI assigned positive values close to 1.0 to zero precipitation records of the dry months as the probability of zero precipitation while SSPI assigned them zero values as the climate norm of the station (see Fig. 4). A careful looking at Fig. 4 also suggests that SPInp even assigned much higher positive values to zero precipitation records at the 1-month time scale as an indication of moderately to very wet conditions. As another discrepancy, SSPI also detected more severe drought conditions than SPI and SPInp at the shorter time scales. Nonetheless, the R between the two indices in Zabol station is higher than 0.99 at longer time scales, suggesting a very strong association between the two indices as observed for Babolsar. This is because the PZP of the time series decreases when the

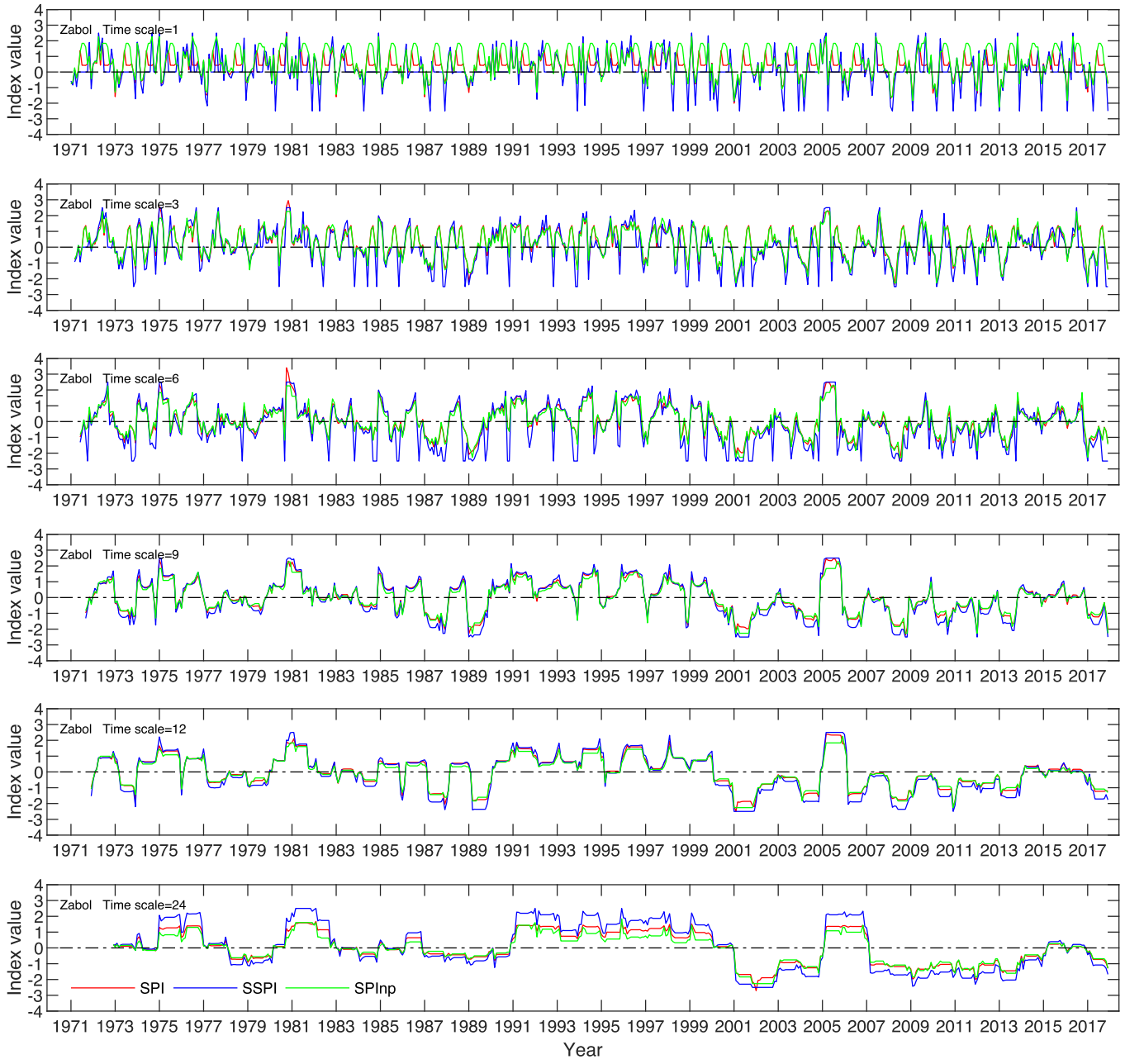

Fig. 4. Comparison of SPI, SPInp and SSPI time series of Zabol station in the southeast of Iran computed at 1-, 3-, 6-, 9-, 12-, and 24-month time scales based upon 1971-2017 period.

time scale exceeds 6-month.

There observed a linear relationship between SPI (SPI_{np}) and SSPI time series at the studied stations and time scales, suggesting that they are consistent in representing dry and wet events at all considered time scales and calendar months, particularly for the wet months. As an example, Fig. 5a-f illustrates the scatter plots of SPI (SPI_{np}) and SSPI time series relative to 1-, 3-, 6-, 9-, 12-, and 24-month time scales at Babolsar station in the north of Iran. As depicted there is a strong linear relationship between SPI (SPI_{np}) and SSPI time series at all the time scales. SSPI shows a similar relationship with both SPI and SPInp which is slightly stronger with SPI, mostly because SPInp assigns SPI values >1.5 to zero summer precipitation values. The scatter plots of the individual months revealed a much stronger linear relationship between SSPI and SPI (SPInp) for the wet months and a weaker relationship for the drier months (not shown). Likewise, Fig. 5g-l depicts the scatter plots of SSPI and SPI (SPInp) for Zabol station at the border with Afghanistan. As is seen, there observed a linear relationship between the indices at all the time scales but with a more dispersed cloud of points around the 1:1 line for the shorter time scales and a more compacted cloud of points for the longer time scales of 9-, 12, and 24 months. The observed dispersion of the cloud of points at the shorter time scales is related to the poor relationship between SSPI and SPI (SPInp) values relative to drier months when both SPI and SPInp assign positive SPI values to zero precipitation records. As an example, at the 1-month time scale, there observed three cases of zero precipitation for which SPI assigned an SPI value >1.5 and SPInp assigned values between 1.5 and 2.0 but SSPI exactly assigned them zero values. Likewise, at the 3-month time scale, there observed two cases of zero precipitation for which both SPI and SPInp assigned an SPI value between 1.0 and 2.0 whereas SSPI exactly assigned them zero values. Due to the existence of a higher number of zero precipitation values in the precipitation series of dry months, the relationship between SSPI and SPI (SPInp) turned to curve linear. Fig. 6

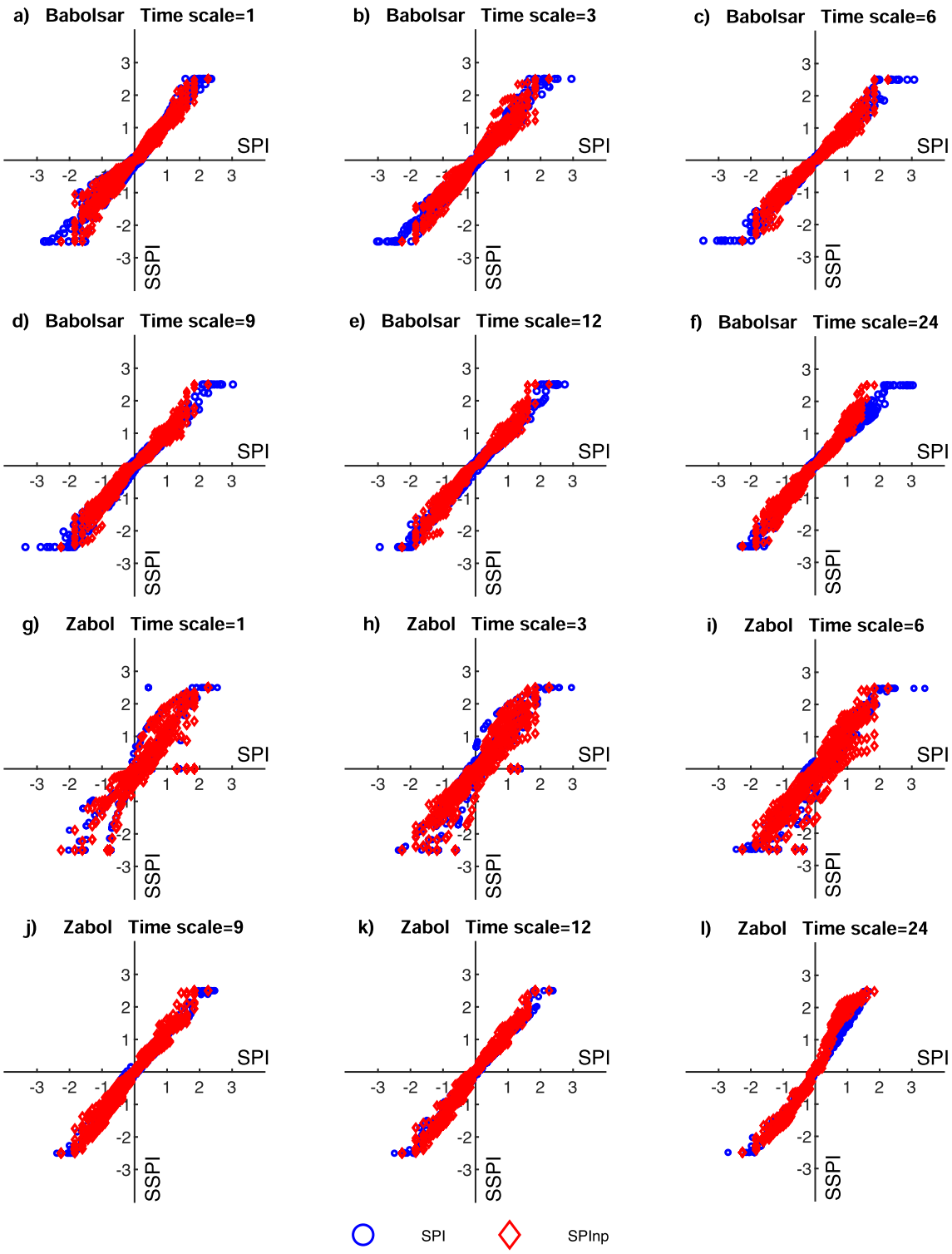

Fig. 5. Scatter plots of SPI (SPInp) and SSPI time series relative to 1-, 3-, 6-, 9-, 12-, and 24-month time scales at Babolsar (a-f) in the north and Zabol (g-l) in the southeast of Iran.

illustrates the scatter plots of monthly indices values and precipitation values for Babolsar station in the north of Iran, with the R values noted in the upper left of each graph. As it is shown, there is a linear trend between the variables (the indices and precipitation) at all individual months. SSPI also shows a very strong correlation with precipitation and highly co-varies with SPI and SPInp at all months, particularly at wetter months. However, this relationship weakens at lower index values for the drier months, indicating a slightly different response of the indices to more severe droughts. This means that there is not a completely linear relationship between the indices at drier months since it turned into a curve linear model at the lower and to some extent at the higher index values which are more profound in February, March, June, July, August, and November at Babolsar station. The reason that the model turns into a curve linear shape at the lower index values is that the SPI tends to show lower values than SSPI for smaller precipitation values. However, Fig. 6 suggests an extremely high agreement between the indices values

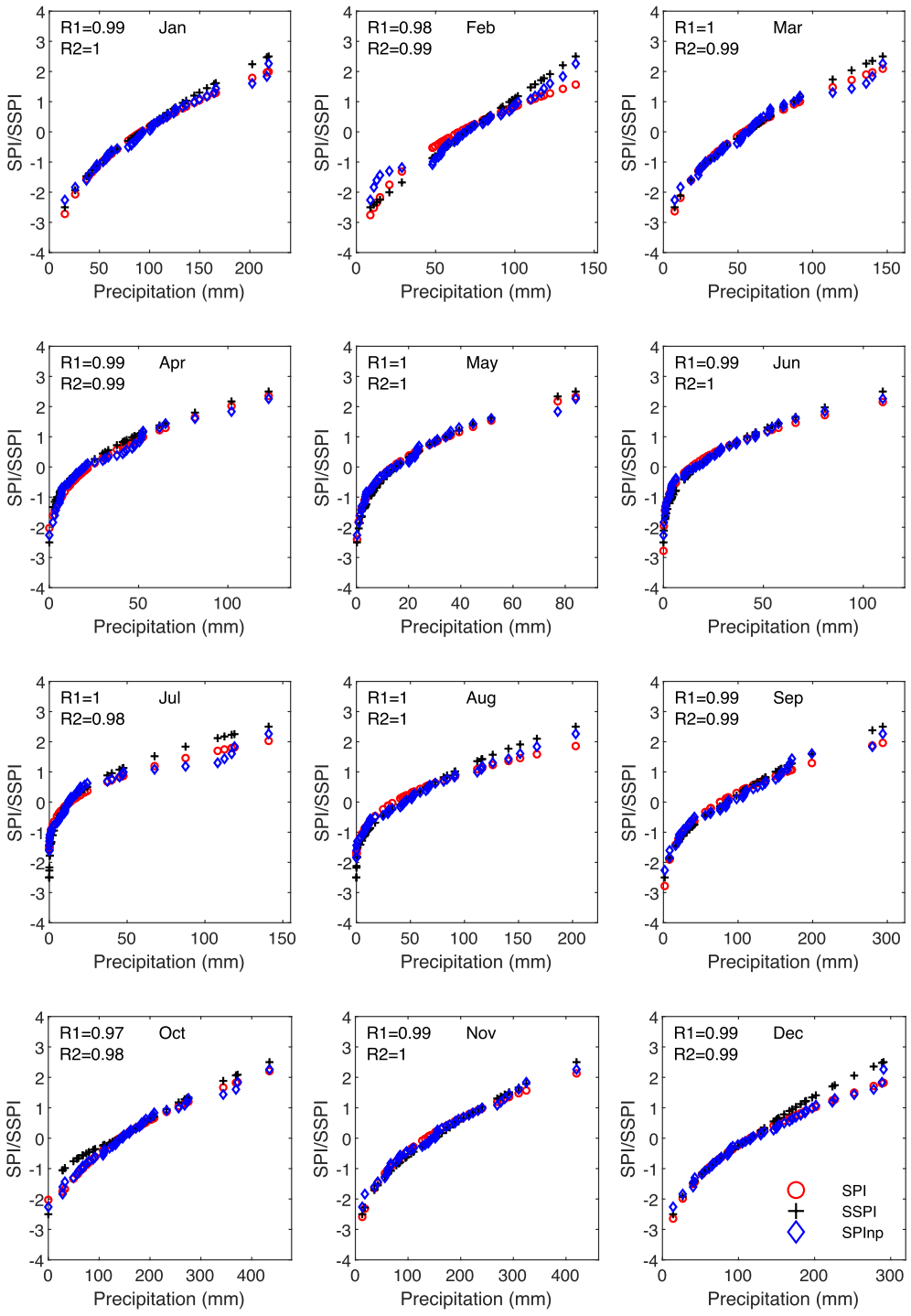

Fig. 6. Scatter plots of monthly SPI/SSPI and precipitation values for Babolsar station in the north of Iran. R1 and R2 denote the correlation coefficient between SSPI and SPI, and between SSPI and SPInp, respectively.

at the central part of the data values. For most of the months, the correlation coefficient between SSPI and SPI (R1) is greater than 0.97, suggesting a very strong association between the indices. A similar pattern is observed for the Zabol station (Fig. 7) but with large differences between SSPI and SPI values from May to November which is because SPI assigns a high probability of zero precipitation (almost >0.5) to zero or negligible precipitation values in the arid and hyper-arid climates. Thus, in locations with distinct dry seasons SPI fails to evaluate the drought condition, especially at short time scales (Wu et al., 2007) when zero precipitation is the climate norm. Therefore when PZP is very high, the equiprobability transformation of precipitation distributions might not be achieved and the resulting SPI time series will not be normally distributed (Blain, 2012). This issue is depicted in the scatter plots of June to August for Zabol station when the SPI assigns very large positive values to zero and negligible precipitation (smaller than 2 millimeters) while SSPI assigns zero values to such precipitation values. This indicates that SSPI presents the most realistic result since the climate norm of the dry season of such locations is almost zero. This can be conceived much better if one notes that precipitation values smaller than 5 millimeters are not effective at all in the presence of very high summer evapotranspiration in dry climates. Despite the observed discrepancies between the two indices at Zabol station, particularly for

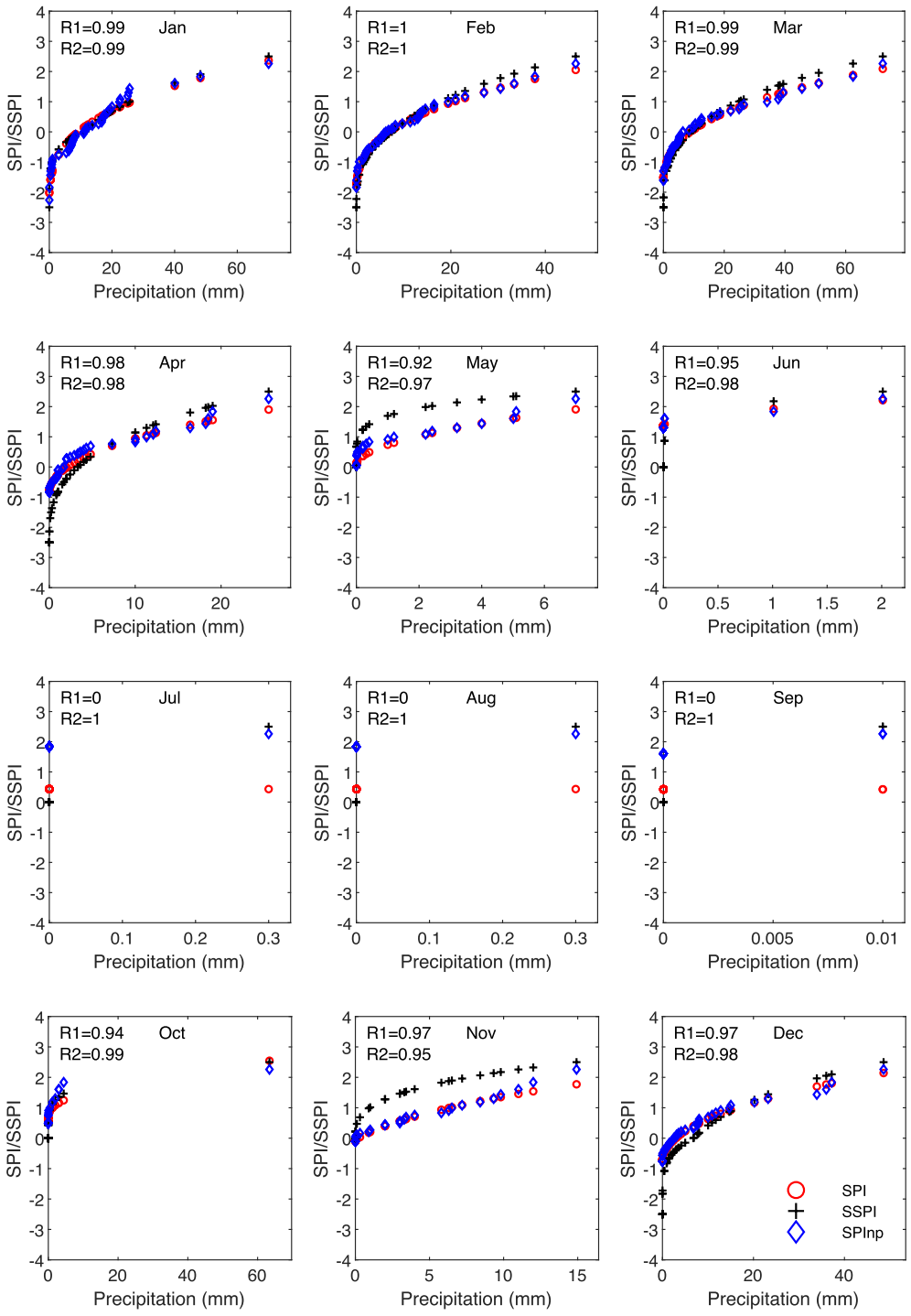

Fig. 7. Scatter plots of monthly SPI/SSPI and precipitation values for Zabol station in eastern Iran. R1 and R2 denote the correlation coefficient between SSPI and SPI, and between SSPI and SPInp, respectively.

the dry months, R is greater than 0.97 from November to April, indicating a very high agreement between SPI and SSPI. However, there observed no correlation between the two indices from July to September when the PZP is approximately 100%. As discussed above, the lower R values of these months are mostly related to the unrealistic SPI values assigned to zero precipitation values. According to Fig. 7, while SSPI correctly assigns zero SSPI values to zero precipitation records of June to October, the SPI unrealistically assigns values close to 1.0 to such precipitation values. The observed perfect linear relationship between the SSPI and precipitation values in these months reveals the mechanism of the third and fourth relationships of Eq. 2 in linearly rescaling precipitation values between zero and 3.0 in the dry season when PZP exceeds 40%. In such cases, i.e., when all or the majority of the time series are zero, the third and fourth relationships of Eq. 2 consider zero precipitation as the climate norm and permit computing SSPI even in the presence of missing data. Differently, it is impossible to compute SPI when there are missing data or an insufficient number of no-zero precipitation records in the time series to fit a distribution function. In such cases, SPI assigns the probability of zero precipitation, which is almost close to 1.0, to all zero precipitation records of the dry months and identifies them as the moderately wet condition which is absolutely a false alarm. Fig. 7 also shows that SPI assigns much higher index values

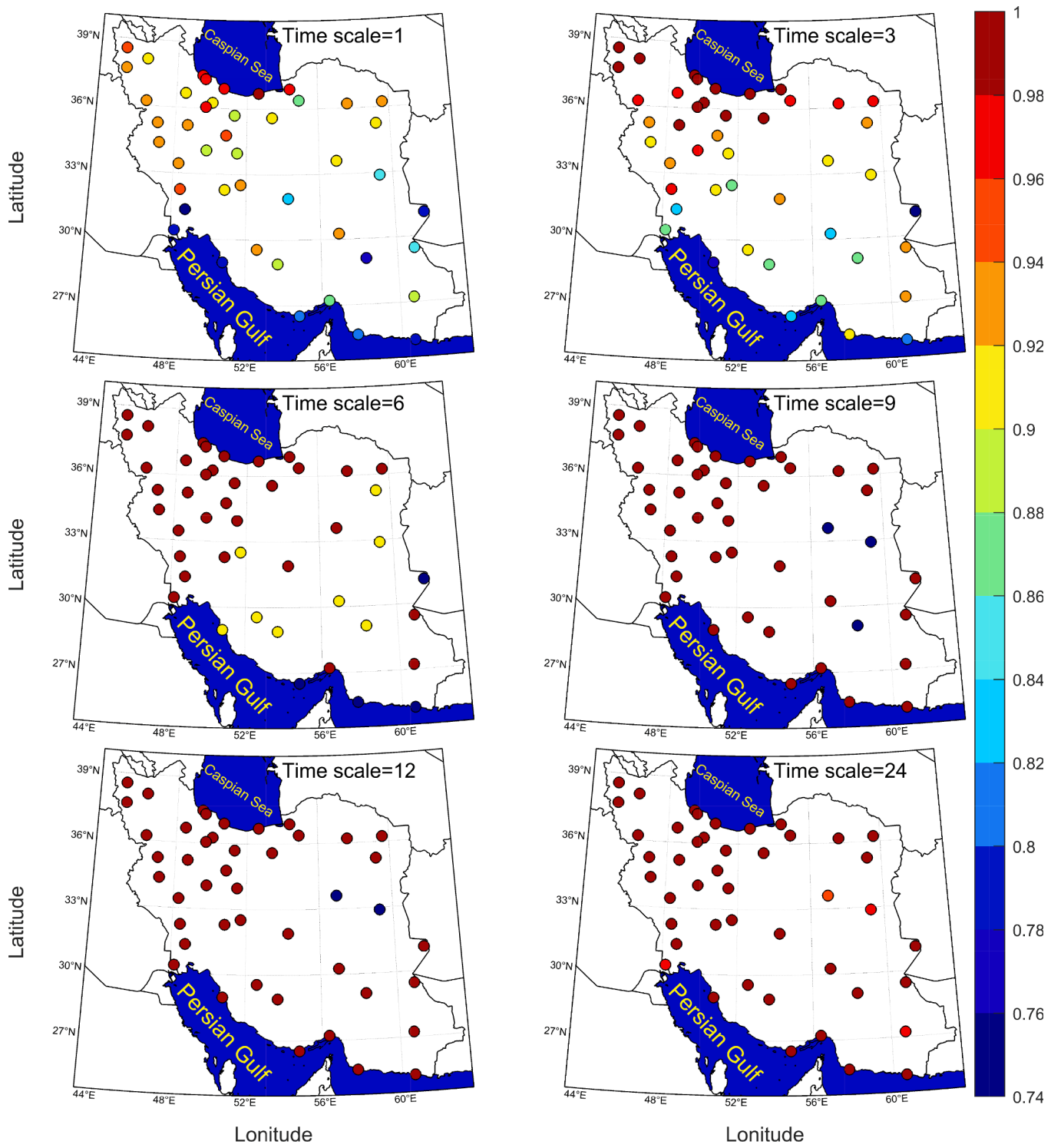

Fig. 8. Spatial variation of the Pearson correlation coefficient (R) across Iran, measuring the association between SPI and SSPI time series at different time scales.

to the lower precipitation of the wetter months than does the SSPI, which means that SPI underestimates the magnitudes of the negative precipitation anomalies of the wetter months of the arid and hyper-arid climates. Comparing the response of SPInp to precipitation records of July to September at Zabol station, it is clear that SPInp performs better than SPI in characterizing the infrequent non-zero precipitation records. As is shown, when no correlation coefficient was found between SPI and SSPI at Zabol station for months July to September (R1), there observed a prefect correlation between SPInp and SSPI denoted by R2. Fig. 8 illustrates how the computed R between SPI and SSPI varies across diverse climates of Iran. At 1-month time scale, R is higher than 0.9 over the coastal areas of the Caspian Sea and most of the stations over the mountainous areas of western and northern Iran that are characterized with either Bsk, Csa, Csb, Cfa, or Dsa climate types. However, it is between 0.74 and 0.9 in southern and southeastern Iran that is dominated by Bwh and Bwk climate types (Raziei, 2017). By comparing the maps, one can notice that R generally increases all over the country by increasing the time scale, particularly at the 3-month time scale, in south of Iran. For the longer time scales, a relatively uniform distribution of R values higher than 0.96 is observed, implying a very high consistency

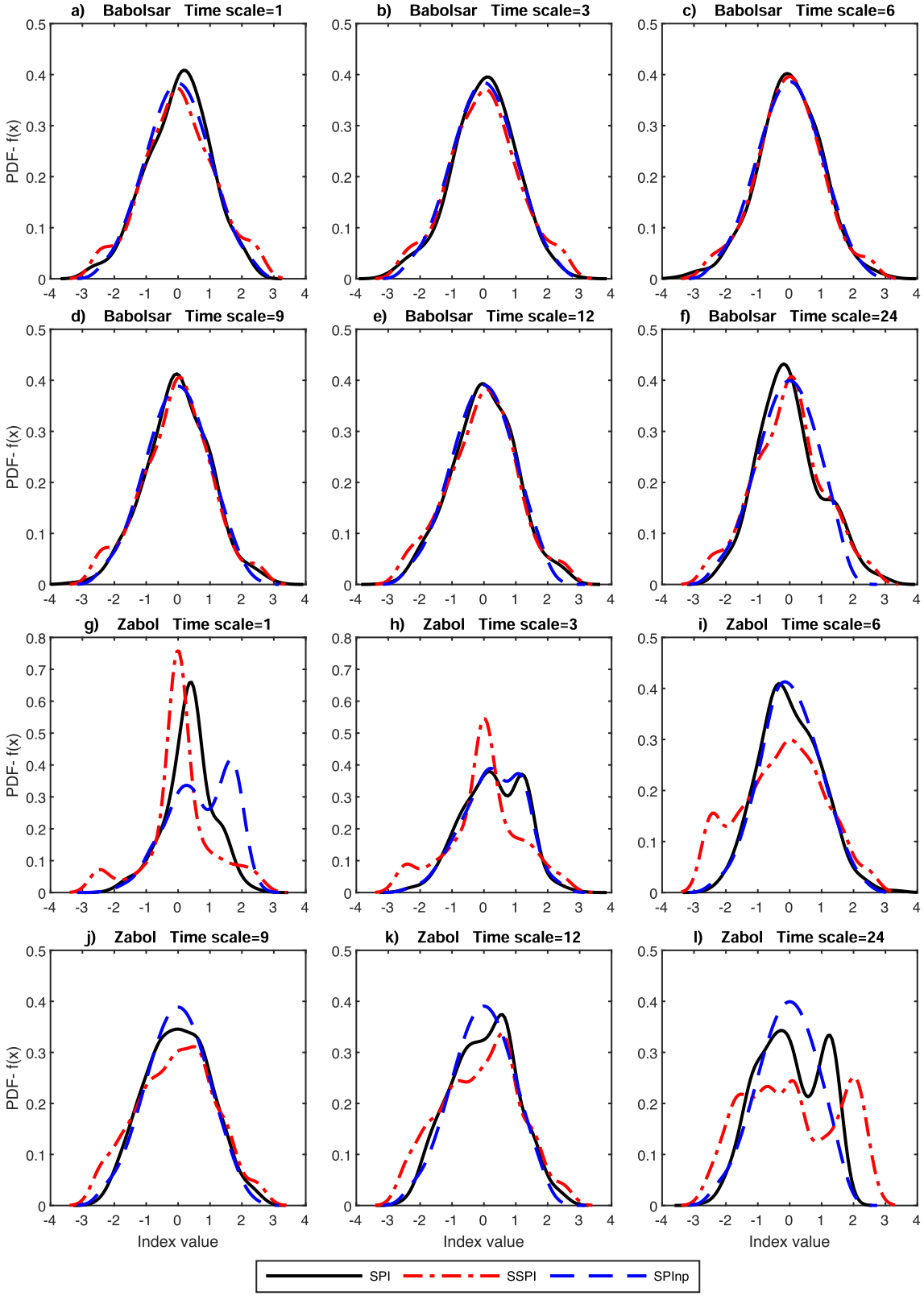

Fig. 9. The PDFs of SPI, SPInp, and SSPI time series relative to 1-, 3-, 6-, 9-, 12-, and 24-month time scales at Babolsar in the north (a-f) and Zabol in the southeast of Iran (g-l).

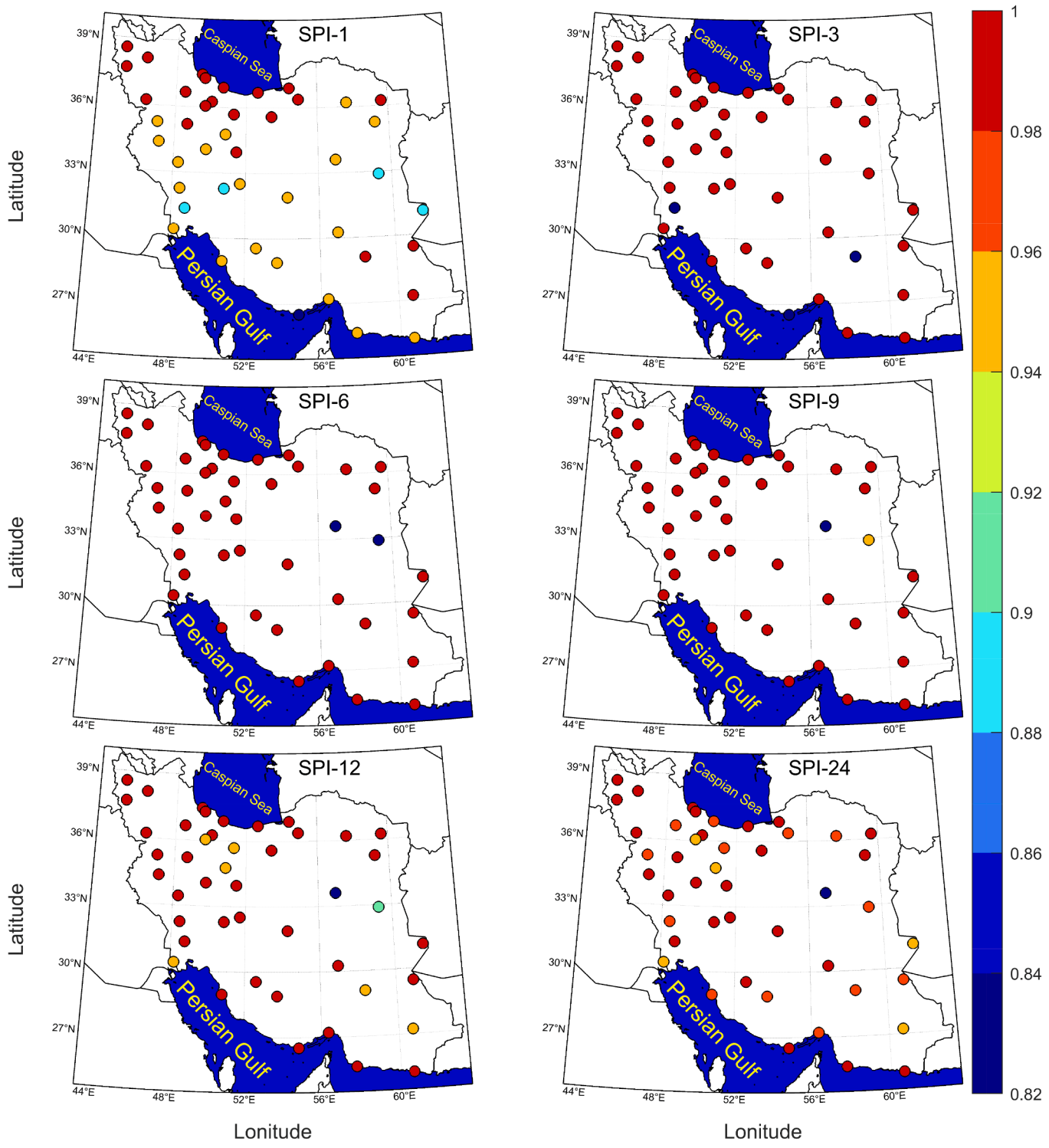

Fig. 10. Spatial variation of S-W test of the SPI time series across Iran computed for different time scales.

between the two indices across the country.

Fig. 9a-f depicts the PDF of the SPI, SPInp, and SSPI time series at Babolsar station computed for different time scales. As it is seen, the PDF of SSPI and SPI (SPInp) time series follow each other reasonably well at all the time scales. Similarly, Fig. 9g-l compares the PDF of SSPI and SPI (SPInp) time series at Zabol station for different time scales. Fig. 9g-l, however, shows considerable discrepancies between the PDF of the indices at 1-, 3-, and 6-month time scales, which is related to different responses of the indices to very large PZPs of the station. Fig. 9g-l suggests that the SPI and SPInp are relatively lower bounded at shorter time scales which is common in regions with low seasonal precipitation totals where precipitation is highly seasonal and heavily skewed. In such areas, SPI behaves very similar to the percent of Normal index in representing precipitation anomalies at shorter time scales and therefore fails in identifying drought occurrences because of non-normally distributed SPI values (Wu et al., 2007) as exemplified in Figs. 3 and 4. Moreover, because of high PZPs in such stations, the SPI and SPInp tend to have their maximum frequencies at SPI value around 1.0 because

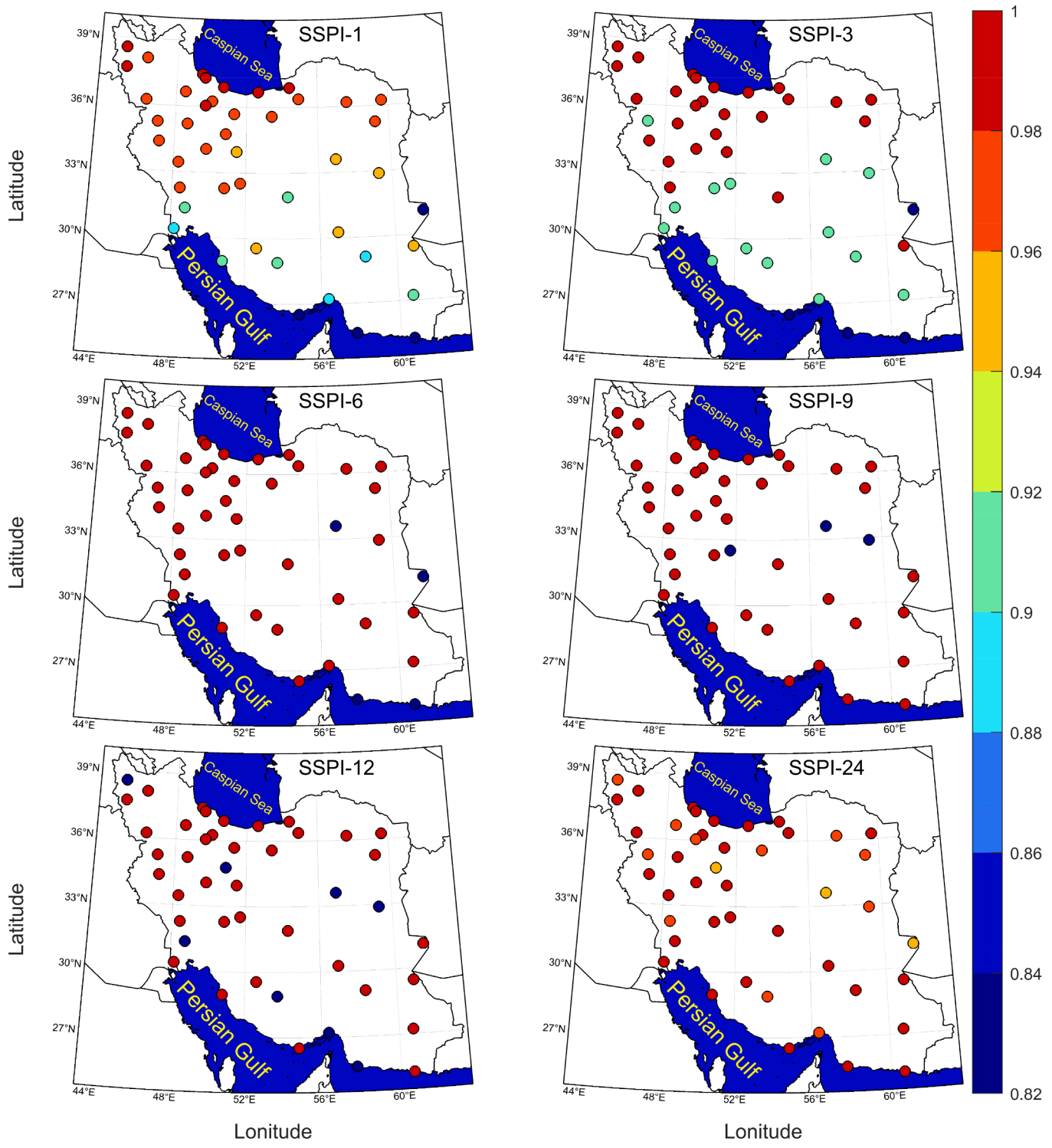

Fig. 11. Spatial variation of S-W test of the SSPI time series across Iran computed for different time scales.

of assigning the probability of zero values to zero precipitation while SSPI maximized exactly at zero value (Fig. 9g-l). Additionally, there observed noticeable differences between SPI and SPInp at Zabol station for shorter time scales, particularly at the 1-month time scale where SPInp assigns much higher positive values to summer season zero precipitation than the SPI (see Fig. 4). The PDFs of the individual summer months showed much narrower bounds of SPI values for shorter time scales at Zabol station. Nonetheless, there is a high consistency between the PDFs of the indices at 9-, 12-, and 24-month time scales for which the PZP is close to zero (Raziei, 2021).

Fig. 10 shows the spatial variation of the S-W test computed for the SPI time series of different time scales across Iran. As is illustrated, for the majority of the stations the S-W test is greater than 0.96 for all considered time scales, particularly those stations distributed across northern and western Iran. This implies that the SPI time series of all considered time scales are normally distributed in most of the studied stations, except for SPI-1 and SPI-3 for which a few stations scattered over the southeastern part of the country show lower S-W test values.

Table 3
Skewness of SPI (SSPI) time series relative to all studied stations and time scales.

Stations	SPI-1	SPI-3	SPI-6	SPI-9	SPI-12	SPI-24
Abadan	−0.5 (−0.2)	−0.4 (−0.2)	−0.2 (−0.1)	−0.2 (−0.0)	−0.3 (−0.0)	−0.8 (0.1)
Ahwaz	−0.5 (−0.2)	−0.5 (−0.2)	−0.3 (−0.1)	−0.2 (−0.1)	−0.2 (−0.2)	−0.4 (0.1)
Arak	−0.5 (−0.3)	−0.1 (−0.1)	−0.1 (0.1)	−0.0 (0.0)	0.0 (0.0)	0.1 (0.0)
Babolsar	−0.2 (0.0)	−0.2 (0.0)	−0.2 (−0.0)	−0.0 (−0.1)	−0.0 (−0.1)	0.4 (0.0)
Bam	−0.3 (−0.2)	−0.4 (−0.2)	−0.4 (−0.1)	−0.5 (−0.0)	−0.4 (−0.1)	−0.5 (−0.1)
BandarAbass	−0.5 (−0.4)	0.2 (−0.0)	0.0 (0.1)	−0.0 (0.1)	0.2 (0.2)	0.1 (−0.1)
BandarAnzali	−0.5 (−0.0)	−0.1 (−0.0)	0.1 (−0.0)	0.2 (−0.1)	0.3 (−0.0)	0.2 (0.1)
BandarLengeh	−0.5 (−0.4)	−0.5 (−0.3)	−0.1 (−0.2)	−0.2 (0.0)	−0.1 (0.0)	0.2 (0.1)
Birjand	−0.8 (−0.3)	−0.5 (−0.1)	−0.7 (−0.1)	−0.5 (−0.1)	−0.5 (−0.1)	−0.6 (0.0)
Bushehr	−0.4 (−0.2)	−0.4 (−0.2)	0.0 (−0.1)	0.1 (−0.0)	0.3 (−0.1)	0.5 (0.0)
Chahbahar	−0.2 (−0.3)	0.1 (−0.3)	0.0 (−0.2)	−0.2 (−0.0)	−0.3 (0.1)	−0.1 (0.0)
Dezful	−0.6 (−0.2)	−0.4 (−0.2)	−0.4 (−0.1)	−0.2 (−0.0)	−0.2 (−0.1)	−0.1 (0.2)
Esfahan	−0.4 (−0.2)	−0.2 (−0.0)	−0.5 (−0.0)	−0.3 (−0.0)	−0.3 (−0.0)	−0.1 (−0.0)
Fassa	−0.5 (−0.3)	−0.1 (−0.1)	−0.2 (−0.0)	0.0 (0.1)	0.1 (0.1)	0.1 (0.1)
Ghazvin	0.0 (−0.0)	−0.1 (−0.0)	−0.3 (−0.1)	−0.3 (−0.0)	−0.4 (0.0)	−0.2 (0.1)
Ghom	−0.5 (−0.2)	−0.2 (−0.1)	−0.2 (−0.0)	−0.0 (0.0)	0.1 (0.1)	0.3 (0.1)
Gorgan	−0.4 (−0.0)	−0.2 (0.0)	−0.4 (0.0)	−0.5 (0.0)	−0.5 (0.0)	−0.4 (0.1)
Hamedan	−0.3 (−0.3)	−0.2 (−0.1)	−0.1 (0.0)	−0.0 (−0.1)	0.1 (0.0)	0.1 (0.0)
Iranshahr	0.2 (−0.4)	0.1 (−0.0)	−0.2 (−0.1)	−0.3 (−0.1)	−0.5 (−0.1)	−0.8 (−0.1)
Jask	−0.3 (−0.3)	0.1 (−0.3)	0.1 (−0.1)	0.0 (0.0)	0.1 (0.0)	−0.0 (−0.0)
Kashan	−0.3 (−0.2)	0.1 (−0.1)	0.2 (−0.0)	0.3 (−0.0)	0.2 (−0.0)	−0.1 (−0.1)
Kerman	−0.6 (−0.2)	−0.2 (−0.0)	−0.3 (0.1)	−0.4 (0.1)	−0.2 (0.1)	0.0 (0.1)
Kermanshah	−0.6 (−0.2)	−0.1 (−0.2)	−0.1 (−0.0)	−0.2 (0.1)	−0.1 (0.1)	−0.1 (−0.0)
Khorramabad	−0.7 (−0.1)	−0.1 (−0.1)	−0.1 (−0.0)	−0.1 (−0.0)	−0.0 (−0.1)	0.1 (−0.1)
Khoy	−0.3 (−0.1)	−0.2 (−0.1)	−0.2 (0.1)	−0.0 (−0.0)	0.1 (−0.0)	0.0 (−0.1)
Mashhad	−0.3 (−0.2)	−0.2 (−0.1)	−0.1 (0.0)	−0.1 (0.1)	−0.1 (0.0)	−0.1 (0.1)
Oroomieh	−0.1 (−0.1)	0.1 (−0.0)	−0.0 (−0.0)	0.0 (−0.0)	0.1 (−0.1)	0.2 (−0.1)
Ramsar	−0.3 (−0.0)	−0.2 (−0.0)	−0.2 (0.1)	0.0 (0.1)	0.2 (0.0)	0.5 (−0.1)
Rasht	−0.3 (−0.0)	−0.2 (−0.0)	−0.1 (0.1)	−0.1 (0.0)	0.0 (−0.0)	0.0 (−0.0)
Sabzevar	−0.4 (−0.2)	−0.3 (−0.0)	−0.4 (0.0)	−0.2 (0.0)	−0.2 (0.0)	−0.3 (0.0)
Saghez	−0.2 (−0.2)	−0.2 (−0.1)	−0.1 (−0.1)	0.0 (−0.0)	−0.1 (0.0)	−0.1 (−0.1)
Sanandaj	−0.5 (−0.1)	−0.2 (−0.0)	−0.3 (−0.0)	−0.2 (−0.1)	−0.2 (−0.1)	−0.0 (−0.1)
Semnan	−0.1 (−0.3)	−0.3 (0.1)	−0.2 (0.0)	0.0 (0.2)	0.0 (0.1)	0.0 (−0.0)
ShahreKord	−0.9 (−0.2)	−0.1 (0.0)	−0.3 (−0.0)	−0.1 (0.0)	−0.3 (0.1)	−0.1 (0.1)
Shahroud	−0.3 (−0.1)	−0.4 (−0.0)	−0.3 (−0.1)	−0.2 (−0.0)	0.0 (0.0)	0.5 (0.1)
Shiraz	−0.5 (−0.2)	−0.2 (0.1)	−0.5 (−0.0)	−0.2 (0.1)	−0.1 (0.1)	−0.3 (−0.0)
Tabass	−0.6 (−0.1)	−0.0 (−0.1)	0.5 (0.2)	0.8 (0.2)	1.0 (0.3)	1.4 (0.3)
Tabriz	−0.4 (−0.1)	−0.2 (−0.0)	−0.1 (−0.1)	−0.1 (−0.1)	−0.2 (0.1)	0.0 (0.0)
Tehran	−0.2 (−0.1)	−0.2 (−0.0)	−0.3 (−0.1)	−0.4 (−0.0)	−0.6 (0.0)	−0.7 (−0.0)
Torbateheydarieh	−0.7 (−0.2)	−0.3 (−0.0)	−0.3 (−0.0)	−0.1 (0.0)	−0.1 (0.0)	0.0 (0.1)
Takestan	−0.0 (−0.1)	−0.3 (−0.0)	−0.2 (−0.0)	−0.4 (0.0)	−0.5 (−0.0)	−0.6 (−0.0)
Yazd	−0.5 (−0.3)	−0.1 (−0.1)	−0.1 (−0.0)	−0.1 (0.0)	−0.1 (0.1)	−0.0 (−0.0)
Zabol	−0.3 (−0.2)	−0.2 (−0.2)	0.3 (−0.1)	0.1 (−0.1)	−0.0 (−0.1)	−0.1 (0.1)
Zahedan	−0.3 (−0.3)	−0.1 (−0.2)	0.0 (−0.1)	−0.0 (−0.1)	−0.0 (−0.2)	−0.5 (0.1)
Zanjan	−0.3 (−0.1)	−0.3 (−0.0)	−0.3 (−0.0)	−0.3 (−0.0)	−0.4 (−0.1)	−0.5 (−0.1)

Fig. 11 also shows a relatively similar pattern of S-W test values for SSPI time series all over the country, particularly at longer time scales. Comparing Figs. 10 and 11, it is evident that the SSPI shows a higher S-W test value for a higher number of stations at the 1-month time scale, particularly over northern and western Iran, indicating that it performs much better than SPI at this time scale all over the country. Differently, at the 3-month time scale, SPI shows higher values than SSPI in southern and eastern Iran. However, by increasing the time scale, the S-W test increases at all the studied stations, and the test values exceed 0.96 at most of the stations, particularly in the northern and western parts of the country. There are also some sporadic stations in central, southern, and eastern Iran with the S-W test lower than 0.96 at longer time scales. By comparing S-W test values of SSPI and SPI time series, it is concluded that both SPI and SSPI time series are asymmetrically distributed at most of the stations and time scales. Nonetheless, the S-W test value of SPI is higher at a few stations, particularly at shorter time scales which is related to the better normalization procedure used in SPI computation despite its failure in passing the normality tests at many stations.

As additional measures required for deciding whether the indices come from a normal distribution, the skewness and kurtosis of SPI and SSPI series relative to all time scales and stations distributed across the country were computed and presented in Tables 3 and 4. As is seen in Table 3, at most of the stations, the skewness of both SPI and SSPI (in parenthesis) relative to all the time scales are comparable and fall within the range of -0.5 and +0.5. However, in almost all of the stations, the skewness of SSPI is much lower than that of SPI at all the time scales, and in most cases, it is close to zero. This difference is particularly more noticeable at Tabass station in central-eastern Iran, specifically for 12- and 24-month time scales. Table 4 also presents the kurtosis of the indices series for all the time scales and stations considered. This Table also revealed that at most of the stations the kurtosis of both SPI and SSPI indices confined between ±3, particularly for larger time scales, indicating that the indices are approximately normally distributed. At most of the stations, the kurtosis of the SSPI is noticeably lower than that of the SPI which is an indication that the tails of the SSPI series are lighter than those of the SPI index. Nonetheless, the computed kurtosis of SPI time series relative to 1- and 3-month time scales is larger than 3 for most of the stations whereas it is smaller than 3 for SSPI, suggesting that the SSPI series are closer to a normal distribution than the SPI series. Fig. 12 illustrates the q-q plots of SPI and SSPI time series relative to 1-, 3-, 6-, 9-, 12-, and 24-month time scales at the two example stations. The q-q plots of Babolsar station (left-hand columns) suggest that both SPI and SSPI indices plausibly come from a normal distribution since the data points fall about the straight line. This is particularly more plausible for the SPI series, however, it seems that the extreme SSPI values slightly violated this assumption. The q-q plots of Zabol (right-hand columns)

Table 4
Kurtosis of SPI (SSPI) time series relative to all studied stations and time scales.

Stations	SPI-1	SPI-3	SPI-6	SPI-9	SPI-12	SPI-24
Abadan	3.0 (3.8)	3.5 (2.9)	2.7 (2.4)	2.5 (2.3)	2.5 (2.3)	3.2 (2.3)
Ahwaz	2.4 (3.3)	3.4 (3.0)	3.1 (2.9)	2.9 (2.8)	3.1 (2.9)	3.5 (2.8)
Arak	4.7 (2.8)	2.9 (2.6)	2.7 (2.6)	2.6 (2.5)	2.6 (2.4)	2.3 (2.2)
Babolsar	2.9 (2.8)	3.1 (2.9)	3.4 (3.1)	3.2 (3.0)	2.9 (2.9)	3.0 (2.8)
Bam	2.6 (3.4)	4.7 (2.7)	3.8 (2.6)	3.5 (2.4)	2.8 (2.4)	2.6 (2.4)
BandarAbass	3.8 (3.7)	3.4 (2.2)	2.9 (2.4)	2.7 (2.4)	2.4 (2.4)	1.9 (1.9)
BandarAnzali	3.6 (2.5)	2.8 (2.6)	2.6 (2.5)	2.8 (2.6)	2.9 (2.6)	2.4 (2.4)
BandarLengeh	2.3 (3.3)	3.4 (3.0)	3.0 (2.6)	2.7 (2.5)	2.7 (2.5)	2.6 (2.6)
Birjand	4.4 (2.9)	3.4 (2.4)	3.1 (2.3)	2.6 (2.1)	2.3 (2.1)	3.1 (2.2)
Bushehr	3.1 (3.6)	3.1 (3.3)	3.4 (2.9)	3.5 (3.1)	3.9 (3.4)	3.2 (2.9)
Chahbahar	2.7 (3.5)	4.0 (2.6)	3.0 (2.5)	3.0 (2.8)	3.5 (2.9)	2.4 (2.4)
Dezful	4.6 (2.9)	3.3 (2.5)	3.0 (2.5)	2.8 (2.6)	2.7 (2.6)	2.3 (2.2)
Esfahan	3.2 (3.2)	2.9 (2.2)	2.8 (2.2)	2.4 (2.2)	2.5 (2.3)	2.5 (2.5)
Fassa	4.5 (3.5)	3.1 (2.3)	3.1 (2.8)	2.8 (2.6)	2.6 (2.5)	2.2 (2.1)
Ghazvin	3.3 (2.4)	3.1 (2.8)	3.4 (2.9)	3.3 (3.0)	3.1 (2.8)	2.5 (2.4)
Ghom	4.6 (2.9)	2.7 (2.4)	2.6 (2.4)	2.4 (2.3)	2.2 (2.2)	1.9 (2.0)
Gorgan	3.5 (2.8)	2.7 (2.6)	3.0 (2.7)	3.1 (2.7)	3.1 (2.7)	2.9 (2.6)
Hamedan	3.9 (3.0)	2.7 (2.5)	2.9 (2.7)	2.8 (2.7)	2.9 (2.8)	3.1 (2.8)
Iranshahr	3.4 (2.9)	2.5 (2.2)	2.5 (2.6)	2.5 (2.5)	2.7 (2.6)	3.1 (2.2)
Jask	3.3 (3.7)	3.4 (3.3)	2.5 (2.5)	2.2 (2.3)	2.2 (2.1)	2.4 (2.3)
Kashan	3.2 (3.3)	3.1 (2.7)	2.8 (2.6)	2.6 (2.4)	2.3 (2.3)	2.5 (2.4)
Kerman	3.7 (2.9)	3.6 (2.5)	3.1 (2.7)	3.0 (2.6)	2.9 (2.7)	2.5 (2.5)
Kermanshah	4.1 (3.1)	3.6 (2.8)	3.1 (2.9)	3.2 (2.9)	3.1 (2.9)	3.0 (2.7)
Khorramabad	4.2 (3.3)	3.1 (2.6)	2.6 (2.5)	2.6 (2.5)	2.6 (2.5)	2.8 (2.7)
Khoy	3.4 (2.6)	2.9 (2.5)	3.0 (2.6)	2.6 (2.4)	2.3 (2.2)	2.5 (2.4)
Mashhad	3.6 (2.8)	3.0 (2.6)	2.6 (2.4)	2.5 (2.4)	2.4 (2.4)	2.9 (2.8)
Oroomieh	3.6 (2.5)	2.5 (2.4)	2.5 (2.4)	2.4 (2.4)	2.6 (2.5)	3.6 (3.4)
Ramsar	3.2 (2.5)	3.0 (2.7)	2.9 (2.6)	2.7 (2.6)	2.4 (2.3)	2.8 (2.7)
Rasht	3.0 (2.6)	2.8 (2.6)	2.8 (2.5)	2.6 (2.5)	2.5 (2.5)	2.8 (2.7)
Sabzevar	4.1 (3.1)	3.5 (2.7)	3.2 (2.6)	2.9 (2.6)	2.6 (2.3)	2.2 (2.2)
Saghez	4.4 (3.0)	3.4 (2.7)	2.9 (2.7)	2.9 (2.7)	3.0 (2.9)	3.3 (3.2)
Sanandaj	3.8 (2.8)	2.7 (2.3)	2.6 (2.4)	2.5 (2.4)	2.4 (2.3)	2.0 (2.0)
Semnan	4.1 (3.0)	3.5 (2.8)	3.3 (2.9)	3.2 (3.0)	3.0 (2.9)	2.2 (2.2)
ShahreKord	5.6 (3.3)	3.2 (2.4)	3.1 (2.6)	2.8 (2.7)	2.8 (2.6)	3.1 (3.0)
Shahroud	3.9 (2.4)	3.8 (2.7)	3.3 (2.8)	3.4 (3.0)	3.3 (3.2)	3.5 (3.3)
Shiraz	3.5 (3.2)	3.5 (2.4)	3.5 (2.7)	2.9 (2.6)	3.0 (2.8)	3.1 (3.0)
Tabass	3.3 (3.2)	3.6 (2.8)	3.4 (2.8)	3.4 (2.7)	3.6 (2.9)	4.3 (3.0)
Tabriz	4.0 (2.5)	3.4 (3.0)	3.1 (3.0)	3.0 (2.8)	2.7 (2.5)	2.5 (2.4)
Tehran	3.7 (2.5)	3.4 (2.9)	3.6 (3.1)	3.3 (2.8)	3.1 (2.5)	3.0 (2.5)
Torbateheydarieh	4.5 (2.7)	3.3 (2.5)	3.1 (2.6)	3.0 (2.6)	2.8 (2.6)	2.2 (2.2)
Takestan	3.2 (2.8)	3.2 (2.6)	2.7 (2.4)	2.6 (2.3)	2.6 (2.1)	2.4 (2.0)
Yazd	3.2 (3.7)	3.5 (3.1)	2.7 (2.6)	2.6 (2.4)	2.4 (2.2)	2.4 (2.4)
Zabol	3.7 (4.3)	2.6 (3.1)	2.9 (2.3)	2.5 (2.4)	2.4 (2.3)	1.9 (1.8)
Zahedan	3.1 (3.1)	3.8 (2.9)	2.9 (2.7)	3.2 (3.0)	3.4 (3.3)	3.8 (3.2)
Zanjan	3.7 (2.4)	3.2 (2.6)	2.9 (2.4)	2.6 (2.4)	2.6 (2.4)	2.8 (2.8)

also show relatively similar patterns for longer time scales. However, for the shorter time scales of 1-, 3-, and 6- month time scales the points do not fall along the straight line, which is attributed to the effects of the higher number of zero precipitation values at these time scales that distort the time series distribution from the normal distribution. The distortion from the normal distribution at Zabol station is more remarkable for the SSPI series where SPI also shows the same response at 1-, 3-, and 6- month time scales as well as the 24-month time scale.

3.2. *Comparing the within class frequencies of the indices*

The frequency of the indices categorized within the nine wetness and dryness classes of Table 1 (middle column) are shown in Figs. 13 and 14 for the two example stations. As it is seen, the frequency distribution of both indices are highly comparable and have a relatively symmetrical distribution at Babolsar in the north of Iran. In all considered time scales, the SPI tends to show slightly higher number of events in the near normal (NN), slightly dry (SD), and slightly wet (SW) classes and fewer events in the extremely wet (EW) and extremely dry (ED) classes. A similar pattern is observed for Zabol at the border with Afghanistan, but with remarkable differences between the indices frequencies at different classes. Fig. 14 demonstrates that the frequency of the NN class of SSPI is higher than that of SPI for 1- and 3-month time scales at Zabol station. The lower frequency of NN class for the SPI is because SPI falsely categorizes the summer months zero total precipitation as MD class that in turn reduced the frequency of the NN class. Moreover, as mentioned before, in such a climate the PDF of SPI is narrow which results in lower frequencies of extreme classes in favor of increasing the frequencies of slightly and moderately wet and dry conditions. This characteristic of SPI decreases the frequencies of VD, ED, VW, and ED classes at the expense of increasing the frequencies of SD, MD, SW, and MW classes, thus, leading to remarkable differences between the two indices regarding the frequencies of the classes. Although the same classification scheme of Table 1 is used to classify the values of both indices, it is not expected that both indices confine well within the defined class limits. Therefore, the observed differences between the frequency distribution of the indices classes dose not point to the inefficiency of either SPI or SSPI if one notes that the considered indices use different standardization as well as classification approaches to classify the index values between the classes. Despite the observed differences between the indices regarding the distribution of their values within the classes, the contingency coefficient and the Cramér's V maps shown in Figs. 15 and 16 show very high values all over the country, suggesting a very high degree of association between the two indices.

The spatial variation of contingency coefficient across Iran demonstrates very high values (CC>=0.9) over the northern part of the country

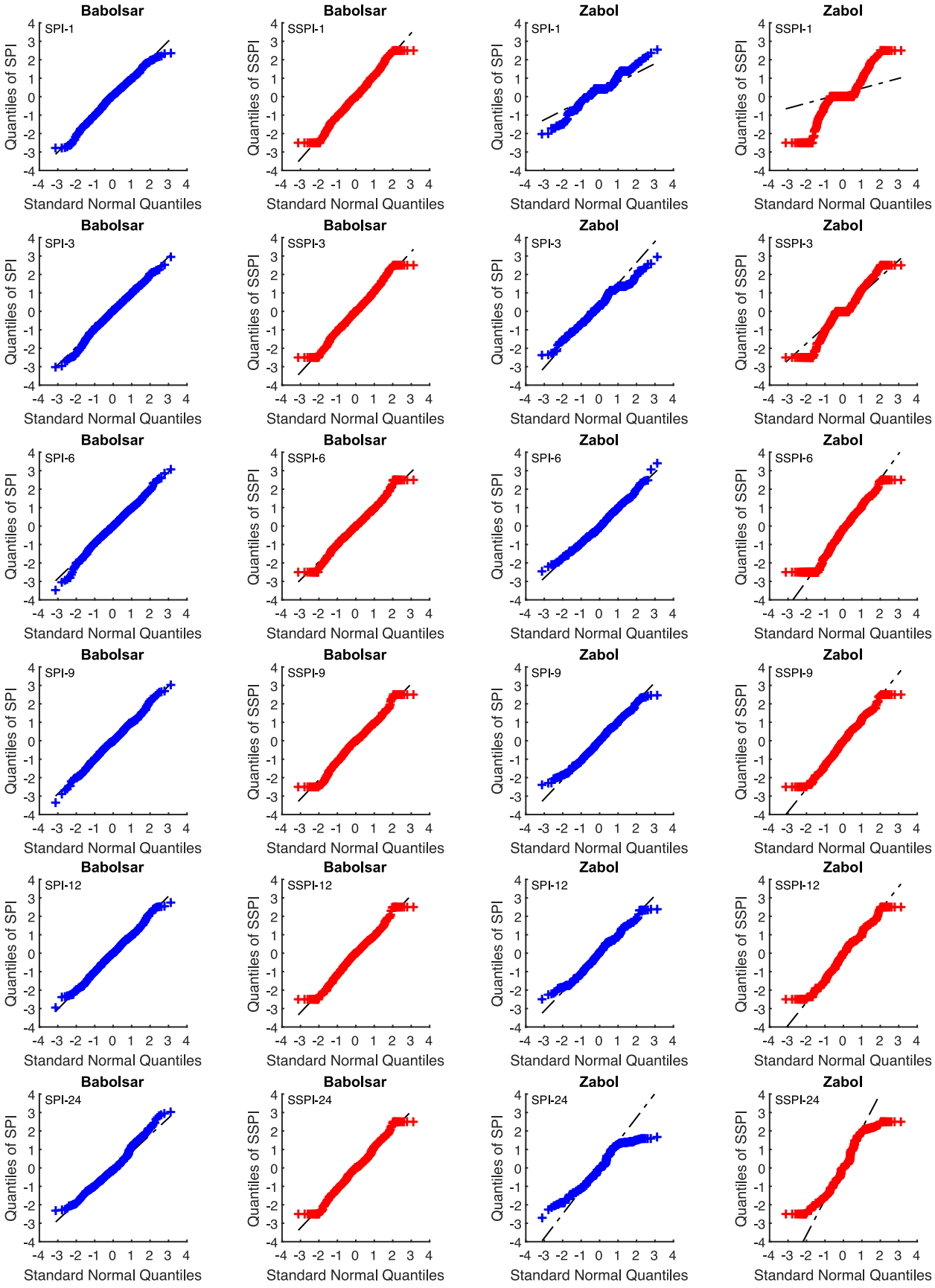

Fig. 12. The q-q plots of SPI and SSPI time series relative to 1-, 3-, 6-, 9-, 12-, and 24-month time scales at Babolsar in the north (two left-hand columns) and Zabol in the east of Iran (two right-hand columns).

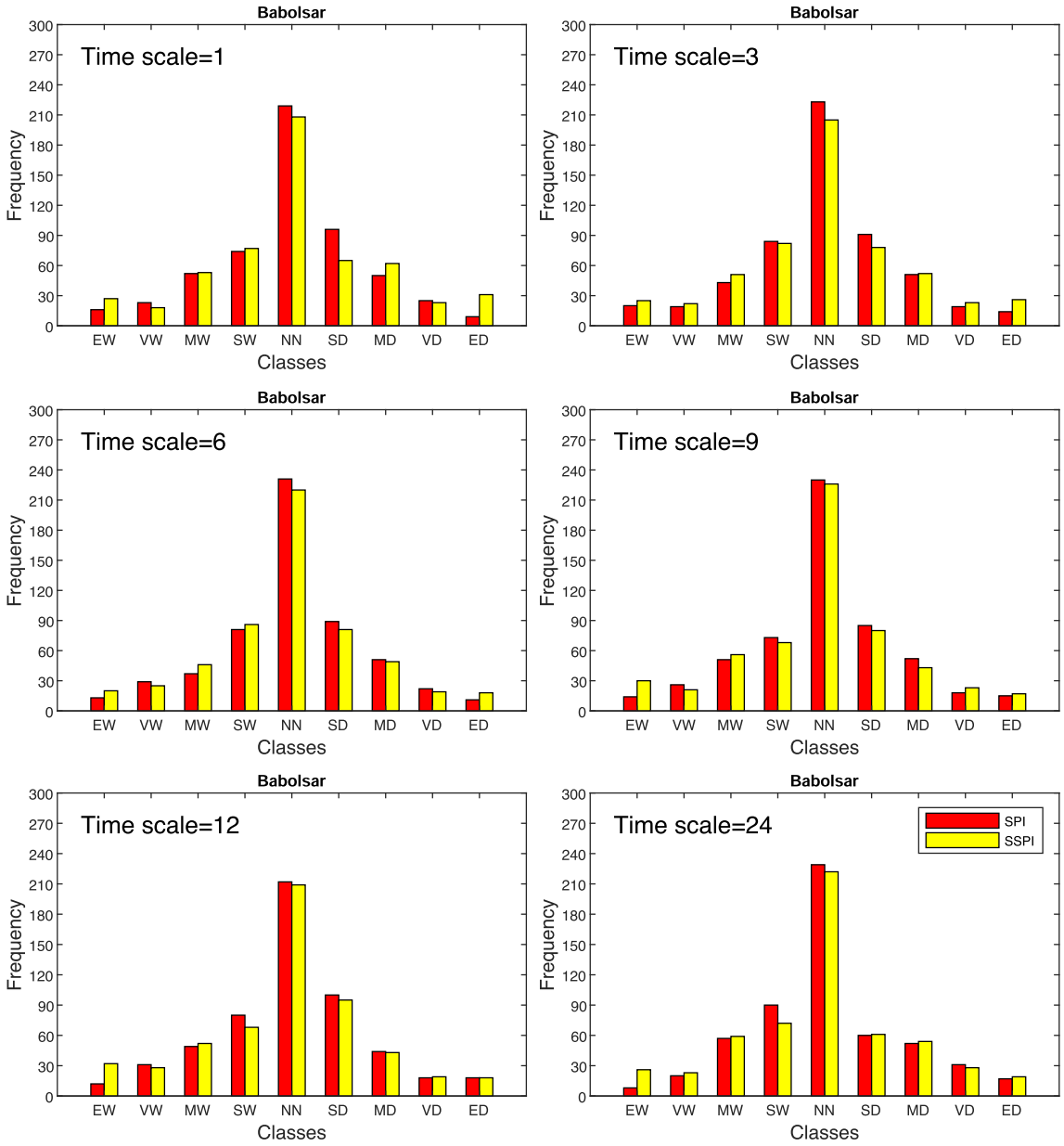

Fig. 13. Frequency distribution of SPI and SSPI classes relative to 1-, 3-, 6-, 9-, 12-, and 24-month time scales at Babolsar station in the north of Iran. The abscissa labels correspond to the short names of the indices categories described in Table 1.

at shorter time scales of 1- and 3-month and lower values ranging between 0.78 and 0.88 over the central, southern and eastern Iran. Considering that CC is the Pearson's correlation coefficient commonly used in comparing nominal values, it suggests a very high agreement between the two indices regarding the distribution of the values between classes even in southern Iran. Based on Fig. 15, the CC value increases with increasing the time scale. Accordingly, at longer time scales, the CC values exceed 0.9 at most of the stations distributed over the country, indicating a much better correspondence between the two indices in classifying the indices values. Fig. 16 also shows a very similar pattern in the spatial distribution of Cramér's **V** statistic across Iran as another measure of association between the indices regarding the frequencies of wet and dry categories. The higher values of the Cramér's **V** statistic is also observed in northern and western parts of Iran and lower ones in the centeral, eastern, and southern parts. The maps of Figures 15 and 16 have more uniform patterns of higher values at longer time scales while a dipole pattern is observed at shorter time scales.

4. Discussion

The comparison of SSPI with SPI and SPInp at the studied stations indicates a strong agreement between the three indices at most of the stations that increases by increasing the time scale. The three indices congruently have captured the widespread historical droughts of 1985-86, 1998-99, 2000-2001, 2007-08, and 2010-11, each of which struck most or some parts of the country with varying severity and duration. As implied by the correlation coefficient greater than 0.98 all over the country, the SSPI fairly explains more than 95% of the time variability of SPI and SPInp at almost all locations. However, there observed some discrepancies between the three indices at shorter time scales, particularly in arid and hyper-arid climates where the dry summer season is very long and the PZP is larger than 50%. As demonstrated in the result section, this discrepancy is mostly due to the inefficiency of SPI and SPInp in characterizing the dry months' precipitation anomalies at stations with very large PZP or when the time series is mostly zero. In such cases, SPI assigned positive values close to 1.0 to zero precipitation

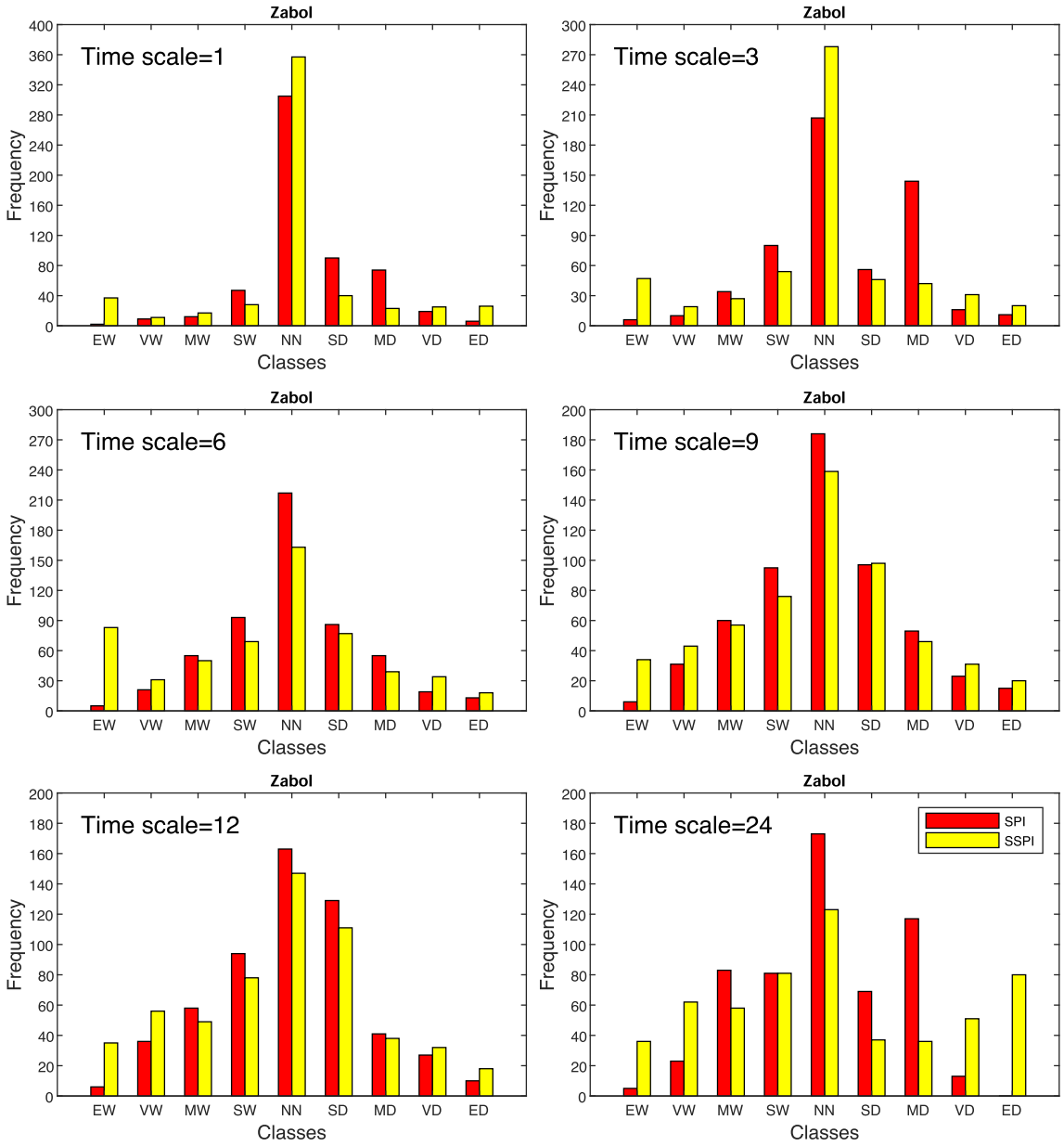

Fig. 14. Frequency distribution of SPI and SSPI classes relative to 1-, 3-, 6-, 9-, 12-, and 24-month time scales at Zabol station in east of Iran. The abscissa labels correspond to the short names of the indices categories described in Table 1.

records of the dry months as the probability of zero precipitation. In cases when most of the time series is zero and the non-zero precipitation values are not adequate to fit a PDF to the data, SPI assigns 1.0 to all data records, including the non-zero precipitation records. This means that the computed SPI values corresponding to such precipitation time series will never fall below 0, and thus, creating the illogical situation that all periods with no detectable precipitation are wetter than is typical for the region (Stagge et al. 2015). Raziei (2021) has examined the center of mass of the zero distribution proposed by Stagge et al. (2015) as an alternative to the historical maximum likelihood of zero precipitation that is commonly used in SPI calculation and found that the SPI values produced using the mean probability of multiple zeros based upon the Weibull plotting position function better maintain the statistical interpretability of the computed SPI. He proved that the method proposed by Stagge et al. (2015) performs much better than the historical maximum likelihood of zero precipitation values in computing SPI in dry climates of Iran where zero precipitation is the typical climate condition of the summer months.SPInp performs much worse than SPI in arid and hyper-arid climates because it specified much higher positive values to zero precipitation records of the dry months. This means that both SPI and SPInp represent the zero precipitation anomalies of the summer season of arid climate as the moderately wet or very wet condition which is a false alarm. This misrepresentation makes both SPI and SPnp unsuitable for computing SPI at short time scales, especially in arid and hyper-arid climates characterized by very high PZP (Raziei, 2021). Nevertheless, a much higher agreement was found between SSPI and SPInp in representing the anomalies of the dry months' precipitation, particularly at 1-month time scale, which is related to the fact that SPI sets aside a positive value >0.5 to both zero and none zero precipitation values while both SPInp and SSPI preserve the magnitudes of the none zero precipitation by allocating relatively similar positive index values to them. This indicates that when most of the time series is zero, which is very common in the arid climate, SPI allocates a fairly low SPI value to non-zero precipitation values. Though SPInp better represents none zero precipitation anomalies of the dry month of the arid and hyper-arid climates than SPI, however, its performance is worse than SPI in representing

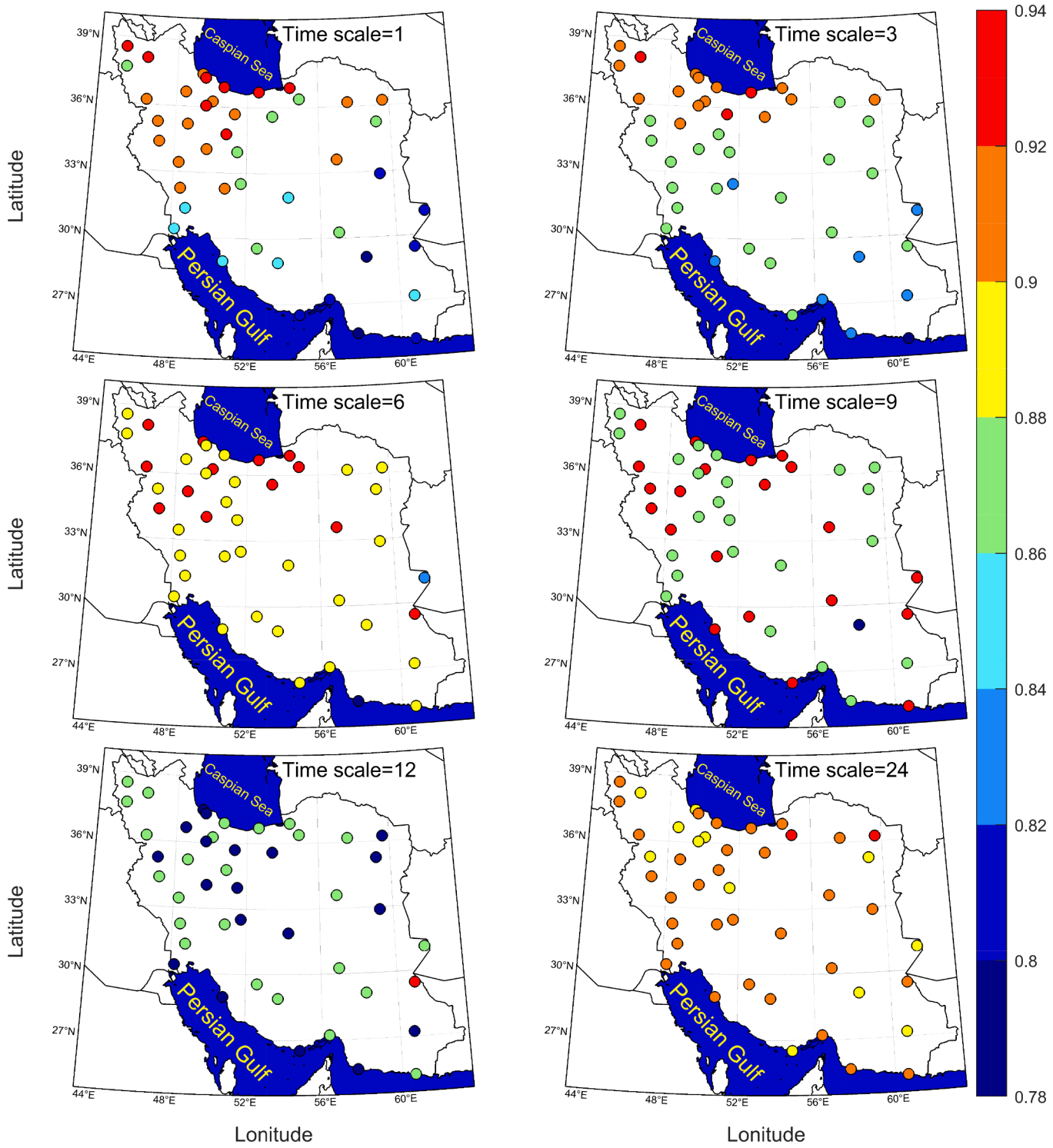

Fig. 15. Spatial variation of contingency coefficient across Iran that measures the association between SPI and SSPI classes at different time scales.

the zero precipitation, as it sets them much higher positive values than does the SPI. Tijdeman et al. (2020) also found that any standardized index derived from non-parametric methods including the kernel density estimation (Vidal et al., 2010) has a large uncertainty bound, and the spread and magnitude of the minimum values of the resulting index do not resemble those expected from a probabilistic index. These shortcomings imply that the SPInp has no advantage over SPI for computing the index at short time scales in arid and hyper-arid climates. More specifically, if one notes that zero precipitation is the climate norm of the dry summer months of the arid and hyper-arid climates, SPInp provides an extremely unrealistic result as it incorrectly sets apart zero precipitation as the moderately wet condition when computing SPI at short time scales. Considering that the accuracy and reliability of SPI calculation depend on the length of the sample at hand, this result suggests that in arid and hyper-arid climates, the SPI values computed with the limited number of non-zero precipitation remained after excluding zero values is substantially uncertain (Hu et al., 2015; Wu et al., 2007). In such a situation, the application of SSPI performs much better results in characterizing aggregated precipitation at shorter time scales. As demonstrated in the result section, SSPI has detected more

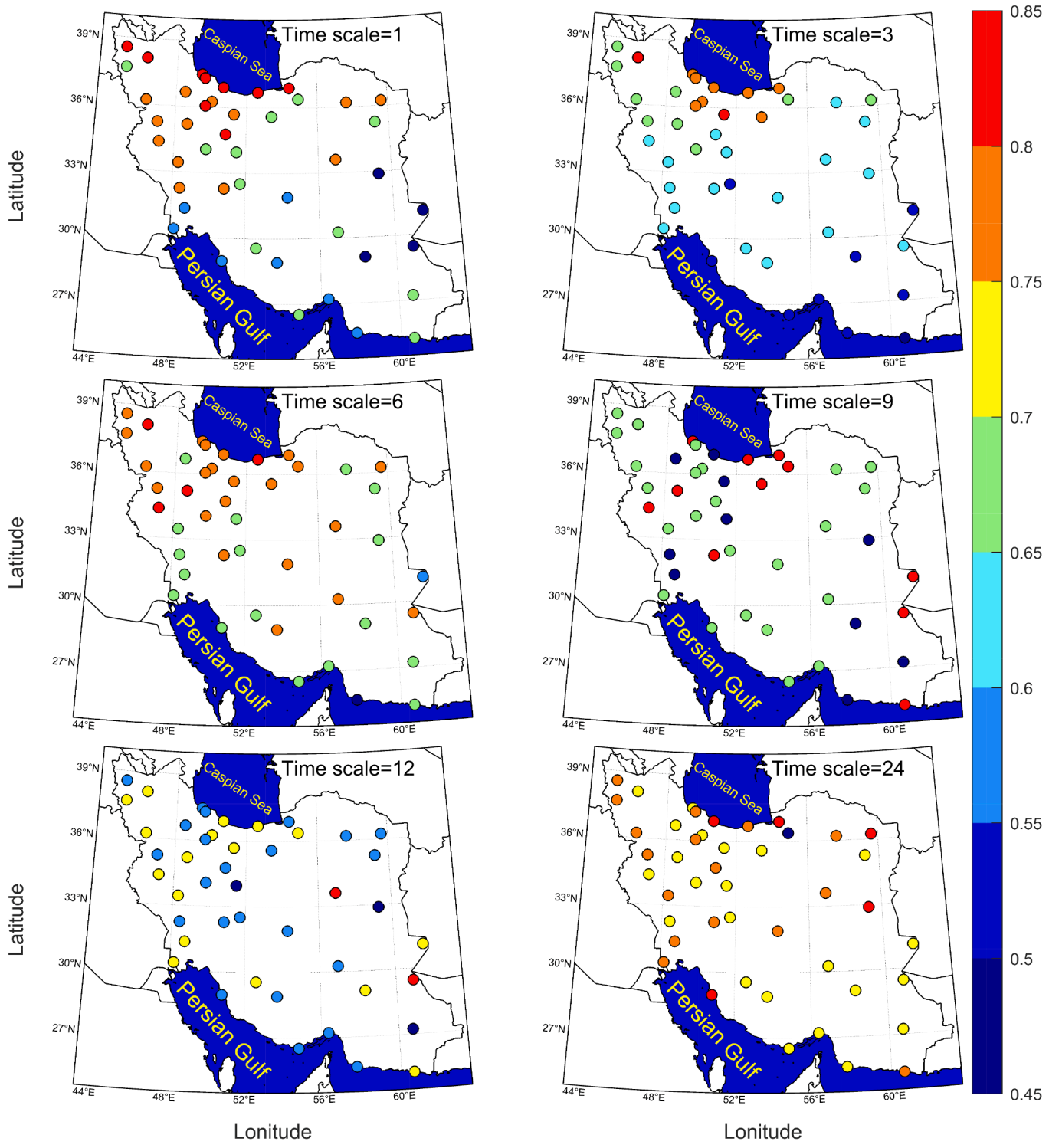

Fig. 16. Spatial variation of Cramér's **V** statistic across Iran that measures the association between SPI and SSPI classes at different time scales.

severe drought and wet conditions than SPI and SPInp which can be partly due to the different scales and transformations used for standardizing the indices values or to the better performance of SSPI in detecting the extreme conditions. This issue needs further examination and it is desirable to be explored in other areas of the world to uncover the strengths and weaknesses of SSPI against SPI.

5. Conclusion

This research introduces the SSPI index that takes into account different time scales and PZP as in the procedure for calculating the SPI index. The SPI and SSPI were then computed for 45 stations distributed over diverse climates of Iran and the resulted time series were statistically compared. The results show a very strong association between the two indices at all considered stations and time scales, particularly at longer ones. The spatial distribution of the correlation coefficient

computed between the two indices depicts large R values across Iran, particularly over northern and western Iran where precipitation is more regularly distributed throughout the year. It is also observed that SSPI well mimics the time behavior of SPI time series at all climatic areas of Iran, more specifically at longer time scales.

Comparing PDFs of SSPI and SPI at two example stations revealed a comparable agreement between the two indices, both being relatively normally distributed at all considered time scales based on the S-W test, skewness, kurtosis, and q-q plots. The spatial distribution of the S-W test computed for all stations and time scales show S-W test values larger than 0.96 at most of the stations over northern and western Iran and lower values in eastern, central, and southern Iran, indicating that both indices are more normally distributed in the former areas where precipitation is less skewed. However, SSPI shows a lower S-W test than the SPI at some stations distributed over south and east of Iran , which is an indication of its higher deviation from the normal distribution than the SPI. By comparing the frequency distribution of the indices values between different dry/wet classes, a strong relation between the two indices are seen. This is indicated by very high values of contingency coefficient and Cramér's **V** statistic at all the stations and time scales considered.

In general, a very strong correspondence between SSPI and SPI is observed regarding the time variability and distribution of the indices values between different dry/wet classes. Nonetheless, the advantages of SSPI against the SPI are its simpler calculation procedure and its ability in allowing for missing data, which is very important for regions where weather data are often incomplete. It also permits computing the index when a large number of or all of the data records are zero values, which is a common feature of arid and hyper-arid climates. This introduces SSPI as the better index applicable to dry climates, where often it is difficult to fit a distribution function to the few non-zero precipitation values for computing SPI, or when computed is less reliable.

Although Olukayode Oladipo (1985), Keyantash and Dracup (2002), and Loukas et al. (2003) have already confirmed the suitability of RAI or a modified version of it (Hänsel et al., 2016) as an alternative to SPI, it is expected that SSPI performs much better than SPI in most parts of the world, particularly in the arid and hyper-arid climates. The SSPI is particularly a superior index for applications in arid and hyper-arid climates where a very large proportion of precipitation values is zero or the length of data records is too short to fit a distribution to the inadequate non-zero precipitation values. Following the auspicious results obtained in this study, evaluating the performance of SSPI in other arid and hyper-arid areas of the world is strongly recommended.

CRediT authorship contribution statement

Tayeb Raziei: Conceptualization, Data curation, Formal analysis, Methodology, Software, Investigation, Visualization, Writing and editing.

Declaration of Competing Interest

The author declares that he has no known competing financial interests or personal relationships that could have appeared to influence the work reported in this paper.

Acknowledgments

Thanks to the two anonymous reviewers for their insightful and invaluable comments that substantially improved the quality of the manuscript.

References

Aksoy, S., Haralick, R.M., 2001. Feature normalization and likelihood-based similarity measures for image retrieval. Pattern Recogn. Lett. 22 (5), 563–582.
Blain, G.C., 2012. Revisiting the probabilistic definition of drought: strengths, limitations and an agrometeorological adaptation. Bragantia 71 (1), 132–141.
Bonaccorso, B., Bordi, I., Cancelliere, A., Rossi, G., Sutera, A., 2003. Spatial Variability of Drought: An Analysis of the SPI in Sicily. Water Resour. Manage. 17, 273–296.
Cramer, H., 1946. Mathematical methods of statistics / by Harald Cramer. Princeton University Press, Princeton.
Domonkos, P., 2003. Recent Precipitation Trends in Hungary in the Context of Larger Scale Climatic Changes. Nat. Hazards 29, 255–271.
Edwards, D.C., McKee, T.B., 1997. Characteristics of 20th Century Drought in the United States at Multiple Times Scales. Atmospheric Science Paper:1–30.
Farahmand, A., AghaKouchak, A., 2015. A generalized framework for deriving nonparametric standardized drought indicators. Adv. Water Resour. 76, 140–145.
Gibbs, W.J., Maher, J.V., 1967. Rainfall deciles as drought indicators. Bureau of Meteorology Bulletin 48.
Guttman, N.B., 1994. On the sensitivity of sample L moments to sample size. J. Climate 7 (6), 1026–1029.
Guttman, N.B., 1998. comparing the palmer drought index and the standardized precipitation index. JAWRA J. Am. Water Resour. Assoc. 34 (1), 113–121.
Guttman, N.B. (1999) Accepting the standardized precipitation index: a calculation algorithm1. JAWRA Journal of the American Water Resources Association 35:311-322.
Guenang, G.M., Kamga, F.M., 2014. Computation of the Standardized Precipitation Index (SPI) and Its Use to Assess Drought Occurrences in Cameroon over Recent Decades. J. Appl. Meteorol. Climat. 53 (6), 2310–2324.
Hänsel, S., Schucknecht, A., Matschullat, J., 2016. The Modified Rainfall Anomaly Index (mRAI)—is this an alternative to the Standardised Precipitation Index (SPI) in evaluating future extreme precipitation characteristics? Theor. Appl. Climatol. 123 (3-4), 827–844.
Hayes, M., Svoboda, M., Wall, N., Widhalm, M., 2011. The lincoln declaration on drought indices: universal meteorological drought index recommended. Bull. Am. Meteorol. Soc. 92, 485–488.
Hayes, M.J., Svoboda, M.D., Wilhite, D.A., Vanyarkho, O.V., 1999. Monitoring the 1996 Drought Using the Standardized Precipitation Index. Bull. Am. Meteorol. Soc. 80 (3), 429–438.
Hu, Y-M, Liang, Z-M, Liu, Y-W, Wang, J, Yao, L, Ning, Y, 2015. Uncertainty analysis of SPI calculation and drought assessment based on the application of Bootstrap. International Journal of Climatology 35, 1847–1857.
Keyantash, J., Dracup, J.A., 2002. The quantification of drought: an evaluation of drought indices. Bull. Am. Meteorol. Soc. 83 (8), 1167–1180.
Khansalari, S., Raziei, T., Mohebalhojeh, A.R., Ahmadi-Givi, F., 2018. Moderate to heavy cold-weather precipitation occurrences in Tehran and the associated circulation types. Theor. Appl. Climatol. 131 (3-4), 985–1003.
Lana, X., Serra, C., Burgueño, A., 2001. Patterns of monthly rainfall shortage and excess in terms of the standardized precipitation index for Catalonia (NE Spain). Int. J. Climatol. 21 (13), 1669–1691.
Lloyd-Hughes, B., Saunders, M.A., 2002. A drought climatology for Europe. Int. J. Climatol. 22 (13), 1571–1592.
Loukas, A., Vasiliades, L., Dalezios, N., 2003. Intercomparison of meteorological drought indices for drought assessment and monitoring in Greece. Proc. Int. Conf. Environ. Sci. Technol. Lemnos Island 484–491.
Mckee T, Doesken N, Kleist J (1993) The relationship of drought frequency and duration to time scales.
Min, S.-K., Kwon, W.-T., Park, E.-H., Choi, Y., 2003. Spatial and temporal comparisons of droughts over Korea with East Asia. Int. J. Climatol. 23 (2), 223–233.
Naresh Kumar, M., Murthy, C.S., Sesha Sai, M.V.R., Roy, P.S., 2009. On the use of Standardized Precipitation Index (SPI) for drought intensity assessment. Meteorol. Appl. 16 (3), 381–389.
Ntale, H.K., Gan, T.Y., 2003. Drought indices and their application to East Africa. Int. J. Climatol. 23 (11), 1335–1357.
Olukayode Oladipo, E., 1985. A comparative performance analysis of three meteorological drought indices. J. Climatol. 5 (6), 655–664.
Palmer, W.C. (1965) Meteorological droughts. US Department of Commerce Weather Bureau Research Paper 45:pp58.
Quiring, S.M., 2009. Monitoring drought: an evaluation of meteorological drought indices. Geography Compass 3, 64–88.
Raible, C.C., Bärenbold, O., Gómez-navarro, J.J., 2017. Drought indices revisited – improving and testing of drought indices in a simulation of the last two millennia for Europe. Tellus A: Dynamic Meteorol. Oceanography 69 (1), 1287492. https://doi.org/10.1080/16000870.2017.1296226.
Raziei, T., 2017. Köppen-Geiger climate classification of Iran and investigation of its changes during 20th century. J. Earth Space Phys. 43, 419–439.
Raziei, T., 2018. A precipitation regionalization and regime for Iran based on multivariate analysis. Theor. Appl. Climatol. 131 (3-4), 1429–1448.
Raziei, T., 2021. Performance evaluation of different probability distribution functions for computing Standardized Precipitation Index over diverse climates of Iran. Int. J. Climatol. n/a. 41 (5), 3352–3373.
Raziei, T., Bordi, I., Pereira, L.S., 2011. An Application of GPCC and NCEP/NCAR Datasets for Drought Variability Analysis in Iran. Water Resour. Manage. 25 (4), 1075–1086.
Raziei, T., Bordi, I., Pereira, L.S., 2013. Regional drought modes in Iran using the SPI: the effect of time scale and spatial resolution. Water Resour. Manage. 27 (6), 1661–1674.
Raziei, T., Bordi, I., Pereira, L.S., Sutera, A., 2010. Space-time variability of hydrological drought and wetness in Iran using NCEP/NCAR and GPCC datasets. Hydrol Earth Syst Sci 14 (10), 1919–1930.

Richman, MB, Trafalis, TB, Adrianto, I, 2009. Missing Data Imputation Through Machine Learning Algorithms. In: Haupt SE, Pasini A, Marzban C (eds) Artificial Intelligence Methods in the Environmental Sciences. Springer Netherlands, Dordrecht 153–159.
Rouault, M., Richard, Y., 2003. Intensity and spatial extension of drought in South Africa at different time scales. Water SA 29, 489–500.
Royston, P, 1992. Approximating the Shapiro-Wilk W-test for non-normality. Statistics and Computing 2, 117–119.
Royston, P, 1993. A Toolkit for Testing for Non-Normality in Complete and Censored Samples. Journal of the Royal Statistical Society : Series D (The Statistician) 42, 37–43.
Seneviratne, SI, Nicholls N, Easterling D, Goodess CM, Kanae S, Kossin J, Luo Y, Marengo J, McInnes K, Rahimi M, Reichstein M, Sorteberg A, Vera C, Zhang X, Rusticucci M, Semenov V, Alexander LV, Allen S, Benito G, Cavazos T, Clague J, Conway D, Della-Marta PM, Gerber M, Gong S, Goswami BN, Hemer M, Huggel C, van den Hurk B, Kharin VV, Kitoh A, Tank AMGK, Li G, Mason S, McGuire W, van Oldenborgh GJ, Orlowsky B, Smith S, Thiaw W, Velegrakis A, Yiou P, Zhang T, Zhou T, Zwiers FW, 2012. Changes in Climate Extremes and their Impacts on the Natural Physical Environment. In: Field CB, Dahe Q, Stocker TF, Barros V (eds) Managing the Risks of Extreme Events and Disasters to Advance Climate Change Adaptation: Special Report of the Intergovernmental Panel on Climate Change. Cambridge University Press, Cambridge 109–230.
Shapiro, S.S., Wilk, M.B., 1965. An Analysis of Variance Test for Normality (Complete Samples). Biometrika 52 (3-4), 591–611.
Shen, S., Dai, Q., Yin, H., Howard, A. (2006) Statistical Analysis of Drought Indices and Drought Monitoring for Alberta, Canada. pp GC41A-1037.
Stagge, J.H., Tallaksen, L.M., Gudmundsson, L., Van Loon, A.F., Stahl, K., 2015. Candidate distributions for climatological drought indices (SPI and SPEI). Int. J. Climatol. 35, 4027–4040.
Stephens, M.A., 1974. EDF statistics for goodness of fit and some comparisons. J. Am. Stat. Assoc. 69 (347), 730–737.
Svensson, C., Hannaford, J., Prosdocimi, I., 2017. Statistical distributions for monthly aggregations of precipitation and streamflow in drought indicator applications. Water Resour. Res. 53 (2), 999–1018.
Svoboda, M, Hayes, M., Wood, D., 2012. Standardized Precipitation Index User Guide. World Meteorological Organization (WMO-No. 1090, Geneva.
Tijdeman E, Stahl, K., Tallaksen, LM.., 2020. Drought Characteristics Derived Based on the Standardized Streamflow Index: A Large Sample Comparison for Parametric and Nonparametric Methods. Water Resources Research 56. https://doi.org/10.1029/2019WR026315.
Tsakiris, G., Vangelis, H., 2004. Towards a drought watch system based on spatial SPI. Water Resour. Manage. 18 (1), 1–12.
Van Lanen, H.A.J., Peters, E., 2000. Effects and Assessment of Groundwater Droughts. In: Vogt, J.V., Somma, F. (Eds.), Drought and Drought Mitigation in Europe. Springer Netherlands, Dordrecht, pp. 49–61.
Van-Rooy, M.P., 1965. A rainfall anomaly index (RAI), independent of the time and space. Notos 14, 43–48.
Vicente-Serrano, S.M., 2006. Differences in spatial patterns of drought on different time scales: an analysis of the Iberian Peninsula. Water Resour. Manage. 20 (1), 37–60.
Vicente-Serrano, S.M., Beguería, S., López-Moreno, J.I., 2010. A multiscalar drought index sensitive to global warming: the standardized precipitation evapotranspiration index. J. Clim. 23, 1696–1718.
Vidal, J.P., Martin, E., Franchistéguy, L., Habets, F., Soubeyroux, J.M., Blanchard, M., Baillon, M., 2010. Multilevel and multiscale drought reanalysis over France with the Safran-Isba-Modcou hydrometeorological suite. Hydrol Earth Syst Sci 14, 459–478.
WMO, 2006. Drought monitoring and early warning: Concepts, progress and future challenges. Meteorological Organization, Geneva, Switzerland WMO-No, p. 1006.
Wu, H., Svoboda, M.D., Hayes, M.J., Wilhite, D.A., Wen, F., 2007. Appropriate application of the standardized precipitation index in arid locations and dry seasons. Int. J. Climatol. 27 (1), 65–79.